

Heat recycling with magnetocaloric materials for sustainable energy conversion

Fengqi Zhang(张烽起) and Yang Ren(任洋)
Citation: Chin. Phys. B, 2026, 35 (**7**): 077502. DOI: 10.1088/1674-1056/ae3693
http://cpb.iphy.ac.cn; http://iopscience.iop.org/cpb

What follows is a list of articles you may be interested in

Strain energy enhanced room-temperature magnetocaloric effect in Mn_5Ge_3

Xiaohe Liu(刘潇贺), Ping Song(宋平), Sen Yao(姚森), Yuhao Lei(雷雨豪), Ling Yang(杨玲), Shenxiang Du(杜深祥), Yiran Deng(邓贻然), and Defeng Guo(郭得峰)
Chin. Phys. B, 2026, 35 (**2**): 027505. DOI: 10.1088/1674-1056/adf6a6

Tuning the magnetocaloric and structural properties of $La_{0.67}Sr_{0.28}Pr_{0.05}Mn_{1-x}Co_xO_3$ refrigeration materials

Changji Xu(徐长吉), Xinyu Jiang(姜心雨), Zhengguang Zou(邹正光), Zhuojia Xie(谢卓家), Weijian Zhang(张伟建), and Min Feng(冯敏)
Chin. Phys. B, 2024, 33 (**12**): 127501. DOI: 10.1088/1674-1056/ad8550

Magnetic and magnetocaloric effect of $Er_{20}Ho_{20}Dy_{20}Cu_{20}Ni_{20}$ high-entropy metallic glass

Shi-Lin Yu(于世霖), Lu Tian(田路), Jun-Feng Wang(王俊峰), Xin-Guo Zhao(赵新国), Da Li(李达), Zhao-Jun Mo(莫兆军), and Bing Li(李昺)
Chin. Phys. B, 2024, 33 (**5**): 057502. DOI: 10.1088/1674-1056/ad1a94

Mechanical and magnetocaloric adjustable properties of Fe_3O_4/PET deformed nanoparticle film

Fengguo Fan(范凤国) and Lintong Duan(段林彤)
Chin. Phys. B, 2024, 33 (**3**): 037502. DOI: 10.1088/1674-1056/acf280

Giant low-field cryogenic magnetocaloric effect in polycrystalline $LiErF_4$ compound

Zhaojun Mo(莫兆军), Jianjian Gong(巩建建), Huicai Xie(谢慧财), Lei Zhang(张磊), Qi Fu(付琪), Xinqiang Gao(高新强), Zhenxing Li(李振兴), and Jun Shen(沈俊)
Chin. Phys. B, 2023, 32 (**2**): 027503. DOI: 10.1088/1674-1056/ac65ef

---

TOPICAL REVIEW — Multiferroicity and multicaloric effects

Heat recycling with magnetocaloric materials for sustainable energy conversion

Fengqi Zhang(张烽起)[†] and Yang Ren(任洋)[‡]

JC STEM Laboratory of Energy and Materials Physics, Department of Physics, City University of Hong Kong, Kowloon, Hong Kong SAR, China

(Received 2 December 2025; revised manuscript received 31 December 2025; accepted manuscript online 12 January 2026)

Solid-state magnetocaloric effects (MCEs) induced by external magnetic fields offer a promising pathway toward sustainable energy conversion technologies, utilizing field-driven temperature changes for efficient solid-state cooling and heating. This review examines magnetocaloric materials (MCMs) in the context of sustainable heat recycling, summarizing representative material systems and key advances from the past decade. The discussion is organized around a materials–applications–mechanism framework to provide a coherent perspective. Finally, we outline existing challenges and future opportunities in the field. Deeper mechanistic insight, combined with advances in manufacturing and the integration of artificial intelligence and machine learning, is expected to accelerate the development of magnetocaloric energy conversion technologies toward practical implementation. Such synergistic progress will accelerate the deployment of these technologies for carbon-neutral heat recycling.

Keywords: sustainable energy conversion, heat recycling, magnetocaloric effect, magnetocaloric materials, refrigeration

PACS: 75.30.Sg, 75.47.Np

DOI: 10.1088/1674-1056/ae3693 **CSTR:** 32038.14.CPB.ae3693

1. Introduction

Sustainable energy conversion is pivotal for modern society, directly addressing the dual crises of climate change and resource depletion.[1,2] On the one hand, global warming and climate change present a fundamental challenge to sustainable development, underscoring the urgent need to adopt zero-emission technologies. Currently, space cooling alone accounts for approximately 37% of global energy consumption,[3] contributing significantly to greenhouse gas emissions and exacerbating climate extremes. This rising demand, exceeding 2000 TWh of electricity annually, equivalent to 2.5 times Africa's total electricity use,[3] highlights the critical importance of improving energy efficiency in cooling systems. Conventional vapor-compression technology, widely used in heating, ventilation, and air-conditioning (HVAC), remains limited by a relatively low Carnot efficiency. Among emerging sustainable alternatives, magnetocaloric energy conversion, one of the most developed solid-state caloric technologies alongside elastocaloric (E_{la}CE), barocaloric (BCE), electrocaloric (E_{le}CE), and multicaloric (M_{ul}CE),[4] offers a promising path forward. With the potential to exceed 60% of Carnot efficiency, it substantially outperforms commercial vapor-compressors, which typically achieve only about 40%.[5] Furthermore, magnetocaloric cooling, which exploits the magnetocaloric effect (MCE), is environmentally benign as it eliminates the need for hazardous refrigerants. On the other hand, magnetocaloric materials (MCMs) can also be applied for thermomagnetic energy conversion, on the basis of the thermomagnetic effect (TME), to convert low-grade waste heat into usable electricity through solid-state, environmentally friendly processes. Solid-state magnetocaloric energy conversion thus holds significant promise for achieving carbon neutrality and decarbonizing the global energy mix. This potential is underscored by major international commitments, such as the European Union's goal for carbon neutrality by 2050,[6] and China's commitment to peak carbon dioxide emissions by 2030 and achieve carbon neutrality by 2060.[7]

MCMs exploit the MCE, which is a physical phenomenon intrinsic to magnetic materials whereby the application or removal of a magnetic field induces a change in magnetic entropy (Δs_m), resulting in an adiabatic temperature change (ΔT_{ad}).[8,9] This mechanism can be directly harnessed for solid-state heating and cooling through adiabatic magnetization and demagnetization cycles. Long-proposed applications based on this effect, such as magnetic refrigeration,[10–12] magnetocaloric heat pumps (for cooling/heating),[13] and thermomagnetic generators for harvesting waste heat,[14,15] have seen substantial development in recent years. Interest in MCE-related research has grown significantly over the past fifteen years.[16] Compared to conventional vapor-compression technology, solid-state magnetocaloric energy conversion offers

[†]Corresponding author. E-mail: fzhan7@cityu.edu.hk

[‡]Corresponding author. E-mail: yangren@cityu.edu.hk

© 2026 Chinese Physical Society and IOP Publishing Ltd. All rights, including for text and data mining, AI training, and similar technologies, are reserved.

exceptional advantages, including potentially higher energy efficiency, environmental friendliness (using no hazardous refrigerants), quiet operation, and enhanced safety.

There are a few review papers focused on fundamental material research associated with MCE and other caloric effects,[9,16–20] thermodynamic perspectives,[5,21] advanced material characterization,[22] and prototypes and manufacturing.[23,24] Following the logic loop of materials-application-understanding, this review comprehensively examines advances in MCMs and their applications (2013–2025). The paper is structured as follows: First, we provide an introduction to magnetocaloric energy conversion, covering: (i) full temperature-range solid-state magnetic refrigeration; (ii) thermomagnetic generators; (iii) micro- and nanoscale applications. The second section reviews recent experimental progress in representative MCMs, focusing on systems exhibiting magneto-elastic and magneto-structural coupling, where the interplay between lattice, magnetic, and electronic degrees of freedom drives first- or second-order phase transitions. Key material families discussed include $(Mn,Fe)_2(P,Si)$-based, $La(Fe,Si)_{13}$-based, NiMn-based magnetic Heusler compounds, and magnetocaloric high-entropy alloys. Finally, we address the major challenges hindering widespread commercialization and highlight emerging opportunities and future perspectives for the development of magnetocaloric energy conversion technologies.

2. Promising applications of MCMs

2.1. Full-temperature range solid-state magnetic refrigeration

Magnetic refrigeration (MR) is widely regarded as the most promising alternative cooling technology and has been extensively studied in recent decades for a variety of application scenarios. Nowadays, the world is facing a looming "cold crunch",[3] driven by the rapidly growing demand for air conditioning, which alone accounts for 40% of the increased electricity use in buildings.[3] This has renewed strong interest in solid-state MR near room temperature (RT) as a replacement for conventional cooling methods. Moreover, as energy storage becomes increasingly critical for integrating renewable sources, cryogenic MR is gaining attention for its potential in liquefying gases such as air, natural gas, nitrogen, hydrogen, and helium, offering a more efficient and cost-effective alternative to traditional high-expense refrigeration techniques.[9] In particular, extreme cryogenic cooling is essential to address helium scarcity, a key resource for space exploration, superconducting science, and quantum technologies.[25] As summarized in Fig. 1 (left), solid-state MR technologies, employing different working materials, can therefore cover the full temperature range from near RT ($\sim$ 300 K) down to sub-kelvin regimes ($<$ 1 K).

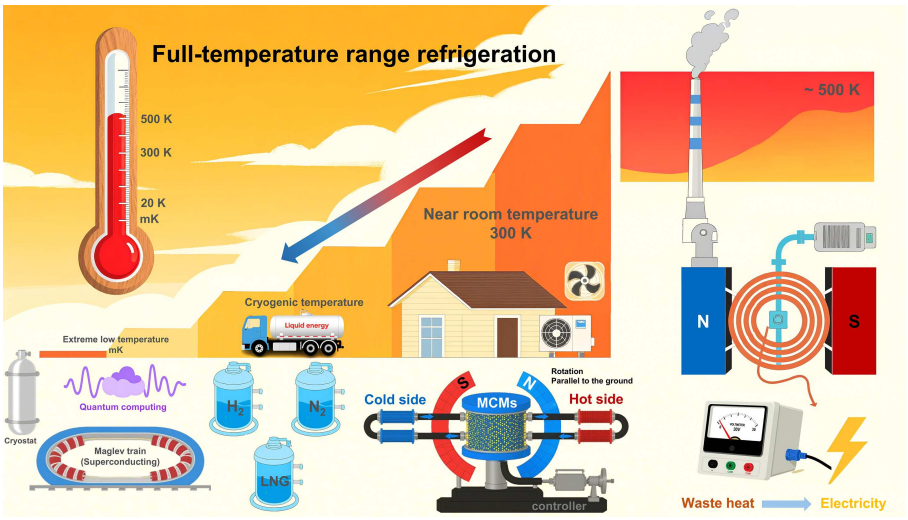


Fig. 1. (Left) Full-temperature range magnetocaloric refrigeration applications from near RT to cryogenic temperature. (Right) High-temperature thermomagnetic generator application for the industrial waste heat recovery.[16] Copyright 2025, Elsevier.

2.1.1. Near room-temperature applications

The development of magnetocaloric applications near RT remained largely unexplored until the 1970s, when the first prototypes based on rare-earth (RE) gadolinium (Gd) were demonstrated.[26,27] Subsequently, research efforts in the early 1990s remained sporadic, with occasional reports of FeRh compounds[28,29] and perovskite-type manganese oxides.[30] In Mn-perovskites[30], a large $|\Delta s_m|$ of 5.5 J·kg^{-1}·K^{-1} was observed with $\Delta\mu_0 H$ of 1.5 T at 230 K. The breakthrough came from the pioneering work on the giant magnetocaloric effect (GMCE), first proposed by Pecharsky *et al.*, near RT in the $Gd_5(Si_2Ge_2)$ material.[10,31,32] Due to the strong FOMT of the phase transition, the $|\Delta s_m|$ of $Gd_5(Si_2Ge_2)$ can reach 18.5 J·kg^{-1}·K^{-1} with $\Delta\mu_0 H = 5$ T at 276 K. More historical details related to the MR near RT can be found in Refs. [23,33]. Numerous MCMs that demonstrate a GMCE

have sprung up, including $(Mn,Fe)_2(P,X)$-based compounds (X = As, Ge, Si),[11] $La(Fe,Si)_{13}$-based materials,[12,34] Ni–Mn-X-based magnetic Heusler compounds (X = Ga, In, Sn, Sb)[35,36] and Mn–M–X (M = Co, Ni and X = Si, Ge) compounds.[37,38] Together with MR, the different emerging refrigeration technologies near RT have been compared.[16,22] Compared with MR, it should be noted that $E_{la}CE$ is limited so far to shape-memory alloys with huge shear strain, and often the reversibility of both $E_{la}CE$ and BCE needs further improvement. On the other hand, avoiding electrical breakdown for $E_{le}CE$ is challenging,[20] and hysteresis and fatigue for $M_{ul}CE$ seem to be key issues for implementing materials into devices.[39] Regardless of many challenges for these solid-state, gas-free cooling/heating technologies, the rapid development of the research activities related to these technologies has gained considerable momentum in recent years.[16,22]

In a complete magnetocaloric cycle, magnetization and demagnetization processes enable the continuous removal and transfer of heat (Q) via a heat-transfer medium (fluid or solid) from the target region. The performance of MCMs is primarily evaluated using two key parameters: Δs_m and ΔT_{ad}. These can be determined through both direct and quasi-indirect measurement methods.[5,9] For the accurate design of MR prototypes, however, data from direct measurements are essential to understand the dynamic magnetocaloric response. The most commonly used (indirect) method to estimate Δs_m and ΔT_{ad} derives from one of the Maxwell relations, yielding $\Delta s_m(T,\Delta H) = \int_0^H \left(\frac{\partial M}{\partial T}\right)_H \mathrm{d}\mu_0 H$ and $\Delta T_{ad}(T,\Delta H) = -\int_0^H \frac{T}{C_p}\left(\frac{\partial M}{\partial T}\right)_H \mathrm{d}\mu_0 H$.[9]

Currently, the most promising magnetocaloric refrigerators capable of achieving a wide operational temperature span are based on the active magnetic regenerative (AMR) cycle, representing a significant advance over passive regeneration systems.[21] The development of MR materials and devices is a global endeavor, involving numerous companies, such as Cooltech Applications (now Magnoric), General Electric (GE), BASF, Vacuumschmelze, Haier, Magnotherm, and Magneto, alongside universities and research institutes across Europe, the United States, China, Japan, and Brazil.[40] For example, in 2014, GE demonstrated a silent magnetocaloric refrigerator for beverage cooling.[41] The following year, Haier, in collaboration with Astronautics, BASF, and TU Delft, unveiled a proof-of-concept wine cooler based on magnetocaloric technology.[42] Meanwhile, Cooltech Applications developed a magnetocaloric refrigerator (MRS400) with cooling power of 400 W, which can well maintain the temperature between 2–5 °C.[43] Moreover, in 2021, Sergiu Lionte *et al*. demonstrated a MR prototype with a >20 °C temperature span, ~ 15 kW cooling power and $\sim 60\%$ Carnot COP.[44] Furthermore, Barbosa *et al.*[45] developed a magnetic wine cooler in 2021, which can refrigerate up to 31 bottles of wine between 10.8–25 °C. The same group reported a magnetocaloric air-conditioning system with 490 W cooling capacity and a 16.8 °C temperature span.[46] Magnotherm, based in Darmstadt, Germany, is a pioneering company developing a new class of MR systems spanning from beverage coolers to cabinet configuration platforms. Recently, the company reported its latest cooler Polaris, which achieved a specific cooling capacity of 131 W/kg, a plug-in COP of 1 and a temperature span of 28.5 K using Gd under 0.8 T.[47] In the past decades, prototype development in MR near RT has been summarized.[24,48] But practical challenges like further improving cooling capacity, enhancing system efficiency, and ensuring reliability should also be addressed.[17]

In addition to space cooling, MR operating near RT shows considerable promise for small-scale thermal storage and management applications.[49–52] For instance, MCMs can be integrated into concentrated solar power and pumped-heat electrical storage systems, often referred to as Carnot batteries.[53] Furthermore, Han *et al.*[54] reported a solar-powered MR desalination device in which solar energy drives seawater evaporation and the MR cycle condenses the steam into fresh water. MR technology can also be coupled with other renewable sources, such as biomass energy.[40] Moreover, near-RT MR offers a viable approach for thermal management of advanced Li-ion batteries during operation.[55] This is exemplified by the EU project "Cool BatMan", which aims to develop a compact hybrid MR proof-of-principle system for battery thermal management in electric mobility.[56] Al-Nimr *et al.* have also modeled the integration of MR with rechargeable batteries in electric vehicles.[57] Beyond these applications, MR near RT is being explored for use in flexible and wearable thermal management devices.[58,59]

2.1.2. Cryogenic applications

For cryogenic applications, the foundational breakthrough was achieved by Giauque and MacDougall, who reached 0.25 K by demagnetizing the paramagnetic salt $Gd(SO_4)_3{\cdot}8H_2O$[60] — a feat for which Giauque was awarded the 1949 Nobel Prize in Chemistry. Advances in cryogenic MR have since reinvigorated interest in the liquefaction of various gases, which serve as efficient energy-storage media. For example, natural gas, a potential hydrogen carrier, is seen as an intermediate step toward decarbonizing the global energy supply. Liquefied natural gas (LNG) at 111 K achieves a density about 600 times greater than that at RT and atmospheric pressure,[61,62] and its consumption is projected to surpass that of oil and coal by 2040.[63] Meanwhile, hydrogen is recognized both as a clean energy carrier and as a cryogenic refrigerant for superconducting technologies.[64] The high density of LNG and liquid hydrogen makes them economically viable for large-scale energy storage and transport via cryogenic tankers,

supporting applications in the energy and chemical industries, fuel-cell electric vehicles, and beyond.

It is known that traditional methods of gas liquefaction can be energy-intensive and expensive, while cryogenic MR gas liquefaction based on AMR could potentially be more efficient and cost-effective,[64,65] and can be complementary to the traditional gas-compression expansion technology. Based on specific conditions, various gases with high economic value, such as helium (He liquefaction temperature is 4.2 K), hydrogen (H_2–20 K), nitrogen (N_2–77 K), oxygen (O_2–90 K), natural gas (CH_4–112 K at 0.1 MPa; 190 K at 4.5 MPa), propane (C_3H_8–231 K), and air, can be sufficiently liquefied at low temperature.[63,66–71] (i) Cooling above 112 K: Several prototypes demonstrate the feasibility of magnetocaloric liquefaction in this range. For instance, Archipley *et al.* reported an AMR refrigerator that successfully liquefied methane, cooling it from 285 K to 135 K using a high-field superconducting magnet.[69] Similarly, Barclay *et al.* utilized a Gd-based AMR cycle to liquefy propane.[70] Liu *et al.* reported that as-cast Nd_2In compounds present a first-order phase transition (FOMT) with negligible thermal hysteresis (also found in Ref. [62]), and showed a large $\Delta s_m = 7.42$ J·kg^{-1}·K^{-1} with a magnetic field change ($\Delta\mu_0 H$) of 2 T and $\Delta T_{ad} = 1.13$ K ($\Delta\mu_0 H = 1.95$ T) at 109 K, making it beneficial for LNG.[63] Notably, some MCMs initially developed for near-RT operation can be effectively tuned for cryogenic use in this range.[72–75] (ii) Cooling between 21 K and 112 K: Significant material discoveries have been made for this temperature regime. Terada and Mamiya reported that holmium (Ho) exhibits GMCE in fields below 1 T between 20 K and 50 K.[66] Guillou *et al.* found the intermetallic compound Eu_2In, which shows a FOMT with strong magnetoelastic coupling and negligible hysteresis. This compound presents maximum Δs_m values of -24.4 J·kg^{-1}·K^{-1} and -28.2 J·kg^{-1}·K^{-1} for $\Delta\mu_0 H$ of 1 T and 2 T (ΔT_{ad} are 2.2 K and 5.0 K). Eu_2In is proposed to outperform all known MCMs in this range, showing promise for nitrogen liquefaction.[68] Recent research has also identified other promising materials, including rare-earth (RE)-based amorphous alloys,[76] intermetallic compounds,[77–79] binary/ternary alloys,[80–82] and classical RE-based MCMs for H_2 liquefaction.[65,83] Efficiently precooling hydrogen from ambient temperature to 77 K using conventional methods is crucial; thus, MCMs with transition temperatures (T_C) in the 21–77 K range are highly desirable to reduce the energy load on MR systems. (iii) Cooling between 10 K and 20 K: This range is critical for hydrogen liquefaction, attracting widespread research interest due to hydrogen's role in sustainable energy.[64,83,84] Initiatives like the EU project "HyLICAL" aim to develop a magnetocaloric hydrogen liquefier prototype.[85] As summarized in Fig. 2, Romero-Muñiz *et al.* categorized MCMs for hydrogen liquefaction into five groups: (1) binary and pseudo-binary intermetallics; (2) ternary intermetallics with main group elements; (3) borides, nitrides, carbides and chalcogenide compounds (RE non-metals); (4) RE oxides; and (5) RE amorphous/high-entropy alloys (HEAs). It is noteworthy that some materials can be modified for multi-target applications spanning ranges (ii) and (iii). For example, HoB_2 compounds exhibit promising cryogenic MCE performance around 15 K, e.g., $\Delta s_m \sim 18$–20 J·kg^{-1}·K^{-1} and $\Delta T_{ad} \sim 5$ K for $\Delta\mu_0 H = 2$ T.[86,87] Liu *et al.* systematically investigated the Δs_m, ΔT_{ad}, and T_C changes of different Laves phases $REAl_2$ and $RENi_2$ materials.[67] Recently, Levinsky and coworkers reported that a novel layered organic–inorganic hybrid coordination polymer $Co_4(OH)_6(SO_4)_2[enH_2]$ (enH_2 = ethylenediammonium) with a second-order magnetic transition (SOMT) can reach $\Delta s_m = -6.31$ J·kg^{-1}·K^{-1} and $\Delta T_{ad} = 1.98$ K for $\Delta\mu_0 H = 1$ T at 10 K $< T_C <$ 15 K.[88] (iv) Cooling below 10 K: Even a reciprocating magnetic refrigerator for helium liquefaction had been designed based on $Gd_3Ga_5O_{12}$ (GGG) materials;[89] however, various oxide-based and intermetallic compounds have been developed rapidly in recent years.[90–93] For instance, Mo *et al.* reported that the ferromagnetic Eu_2SiO_4 compound showed a record $\Delta s_m \sim 21.6$ J·kg^{-1}·K^{-1} for $\Delta\mu_0 H = 1$ T at around 6 K, alongside good thermal conductivity, making it highly relevant for liquid helium production.[94] Li and coworkers reported that RE_2ZnMnO_6 (RE = Gd, Dy and Ho) perovskites have tunable MCE performance between 6 and 10 K.[90] A brief material review can be found elsewhere.[95] Beyond helium liquefaction, achieving ultralow temperatures (< 1 K) is critical for fundamental research, including quantum science and deep-space exploration. Here, helium-free adiabatic demagnetization refrigeration (ADR) presents a promising alternative to traditional ^{3}He adsorption and ^{3}He/^{4}He dilution refrigeration.[64,96,97] For instance, NASA has developed the concept of a continuous ADR system capable of reaching temperatures of 50 mK or lower.[98] A significant challenge, however, lies in the limitations of conventional hydrated paramagnetic salts, which suffer from low magnetic entropy density, poor stability, low thermal conductivity, and long thermal relaxation times. Consequently, recent research has focused on developing alternative materials without crystal water to overcome these drawbacks, e.g., RE oxides,[99–102] metallic ion crystals,[103–105] and Co-based frustrated quantum magnets.[25] As shown in Figs. 2(b) and 2(c), Hu *et al.* found that in orthorhombic $EuCl_2$, record-high values of $\Delta s_m \sim 74.6$ J·kg^{-1}·K^{-1} (1.8 K) at $\Delta\mu_0 H = 5$ T (approaching 96% of the theoretical limit (77.5 J·kg^{-1}·K^{-1})) and $\Delta s_m \sim 36.8$ J·kg^{-1}·K^{-1} at $\Delta\mu_0 H = 1$ T were achieved.[106] In Figs. 2(d) and 2(e), Li and coworkers reported that the rare-earth fluoride, NH_4GdF_4, can achieve $\Delta s_m = 38$ J·kg^{-1}·K^{-1} and $\Delta T_{ad} = 1.1$ K at an

initial temperature of 1.8 K with $\Delta\mu_0 H = 1$ T, where the Δs_m value is greater than all reported results and 9 times higher than the benchmarked $Gd_3Ga_5O_{12}$.[107] Zhang *et al.* reported that the Gd_2CuTiO_6 double perovskite oxide materials have $\Delta s_m \sim 51.4$ J·kg^{-1}·K^{-1} for $\Delta\mu_0 H = 7$ T, which surpasses the commercialized benchmarked refrigerant GGG with $\Delta s_m \sim 38.3$ J·kg^{-1}·K^{-1} at the same field change.[101] Long and coworkers studied $LiGd_{0.1}Yb_{0.9}F_4$ and Gd–Yb–F materials, which are potential candidates for water-free sub-Kelvin-temperature magnetic refrigerants.[104,105] Su and coworkers found that $Na_2BaCo(PO4)_2$ materials with competitive volumetric entropy density, which results from spin supersolidity and the high density of magnetic ions, could be interesting for very low temperature applications below 100 mK.[25]

In a short conclusion, MR development in the full-temperature range has made significant progress in recent years, showcasing the potential of this technology as a sustainable and efficient cooling solution for both cryogenic and near-RT applications.

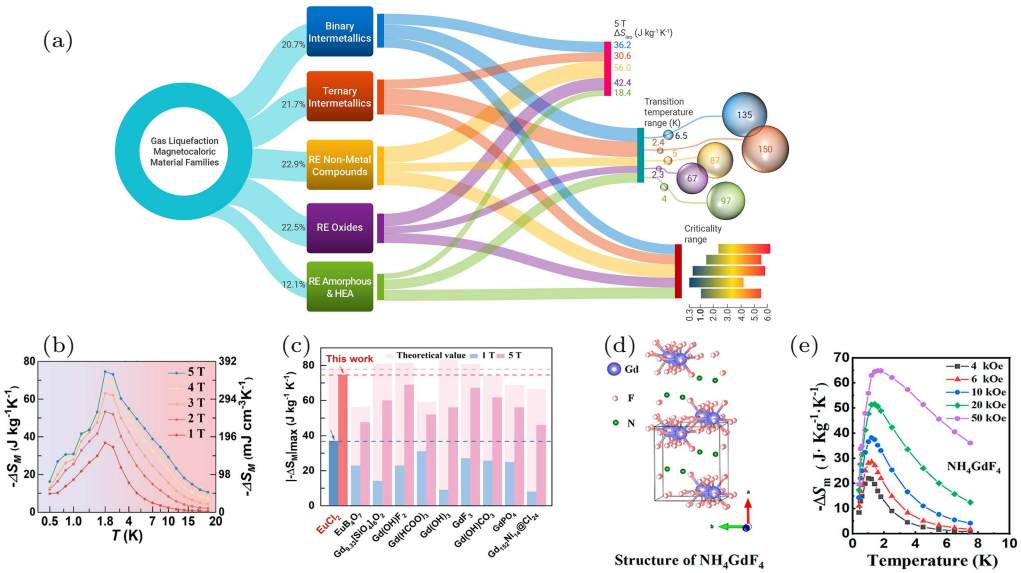


Fig. 2. (a) Cryogenic MCMs for hydrogen liquefaction with critical material parameters. Reproduced under the terms of the CC BY license,[84] Copyright 2023, Author(s). (b) Calculated Δs_m for $EuCl_2$. (c) Comparison of $|\Delta s_m|$ for $EuCl_2$ with other cryogenic MCMs. (d) Crystal structure of NH_4GdF_4. (e) Calculated Δs_m for NH_4GdF_4. (b)–(e) are reproduced with permission.[106,107] Copyright 2024 and 2025, ACS.

2.2. Thermomagnetic applications

Globally, more than 60% of all energy produced is dissipated as waste heat, of which approximately 65% is low-grade waste heat with temperatures below 500 K.[108] Current technologies for harvesting such low-grade thermal energy primarily rely on pyroelectric, thermoelectric (TE), or thermomagnetic effects. However, the efficiency of thermoelectric generators, based on the Seebeck effect, decreases significantly as the temperature difference narrows, with coefficients of performance (COPs) falling below 0.5 for temperature spans of about 20 K.[109] It is therefore essential to explore alternative approaches for converting low-grade waste heat into usable mechanical or electrical energy, as illustrated in Fig. 1 (right). The thermodynamic cycle underlying thermomagnetic energy conversion is shown in Fig. 3(a). This cycle can be implemented in devices such as: (i) thermomagnetic motors (also called "Curie wheels", Fig. 3(b)), (ii) mechanical oscillators (Fig. 3(c)), and (iii) static thermomagnetic generators (Fig. 3(d)). In these systems, thermomagnetic materials function as thermal switches that modulate magnetic flux in response to a temperature gradient.[110] The differences between MCE and TME technologies have been summarized.[16] Currently, the energy conversion efficiency of thermomagnetic devices still needs to be improved further.[15] More details of the mechanisms have been introduced in Refs. [16,111]. Thermomagnetic materials (TMMs) for practical applications should generally possess several fundamental properties: they should be soft magnetic materials with low remnant magnetization, feature a tunable Curie temperature (T_C), exhibit high thermal conductivity for rapid thermal switching, be low-cost and non-toxic, and contain minimal amounts of critical raw materials. For thermomagnetic generator (TMG) applications specifically, promising candidate materials are further characterized by: (i) a critical temperature above room temperature, (ii) a large change in magnetization (ΔM) under low heat input (Q), and (iii) a high derivative $\mathrm{d}M/\mathrm{d}T$, which promotes efficiency in systems with low specific heat.

Recently, different linear thermomagnetic[113] and rotary thermomagnetic motors[114] have been developed. For instance, utilizing Gd spheres, a designed linear thermomagnetic motor can achieve a power of 0.41 W at a frequency of 0.5 Hz.[113] And the rotary thermomagnetic motor with TMMs (Mn_2FeSn) can produce a power of 88 W with a power density of 27 kW/m^3.[114] The rotary thermomagnetic mo-

tor with Gd developed by Swiss Blue Energy can produce up to 1 kW of power.[115] Moreover, different devices utilizing mechanical oscillators have been demonstrated, which basically include a vibrating cantilever, a TMMs film, a permanent magnet, and an induction coil. When the cantilever is bent due to the temperature-driven phase transition, the mechanical energy of the vibrating cantilever can then be converted into electrical energy by the coil. In 2016, Gueltig *et al.* demonstrated an efficient thermomagnetic oscillator using a resonantly actuated Ni–Mn–Ga Heusler film, achieving a notable power density of 118 mW·cm^{-3}.[14] Subsequent work by Joseph *et al.* investigated the influence of film thickness and device footprint on the power and efficiency of such Ni–Mn–Ga-based oscillators.[116] They further optimized the Gd-film-based thermomagnetic oscillator (40 μm thickness) with maximum $\Delta M/\Delta T$ of 2.3 Am^2·kg^{-1}·K^{-1} at 19 °C and operated at frequencies up to 105 Hz.[117] Ramanujan *et al.*[118,119] employed the $(MnNiSi)_{0.7}(Fe_2Ge)_{0.3}$ material, with a transition temperature between 120–150 °C, for the thermomagnetic oscillator, capable of generating up to 10 V per cycle and 15 mA, storing sufficient energy in a capacitor to power an LED. Key parameters for small-scale oscillators have been summarized in subsequent work.[118] Strategies to improve electrical energy collection have also been[120] explored. For instance, piezoelectric polyvinylidene difluoride (PVDF) has been incorporated into cantilever designs. Interestingly, the mechanical motion can be converted into electricity combining the TME (bulk Gd) and the triboelectric conversion.[121] A maximum voltage, current, and power density of 79 V, 2.6 μA, and 18 mW·m^{-2}, respectively, was achieved in a cold- and hot-sides temperature of 30 °C and 65 °C.[121] Such oscillators are promising for applications including wireless computing systems, data storage servers, and the Internet of Things (IoT). Research has also advanced in the area of static TMGs, with various materials being developed and tested. These include 3d/4f pure metals (Co, Fe, Ni, Gd, Tb, Dy, Ho, Er),[117,122,123] $(Mn,Fe)_2(P,As)$,[112] NiMn-based Heusler alloys,[14,124,125] $Gd_5(Si,Ge)_4$,[125] and $La(Fe,Si)_{13}$[15,125–127] compounds. Recent progress in static TMGs is summarized as follows.

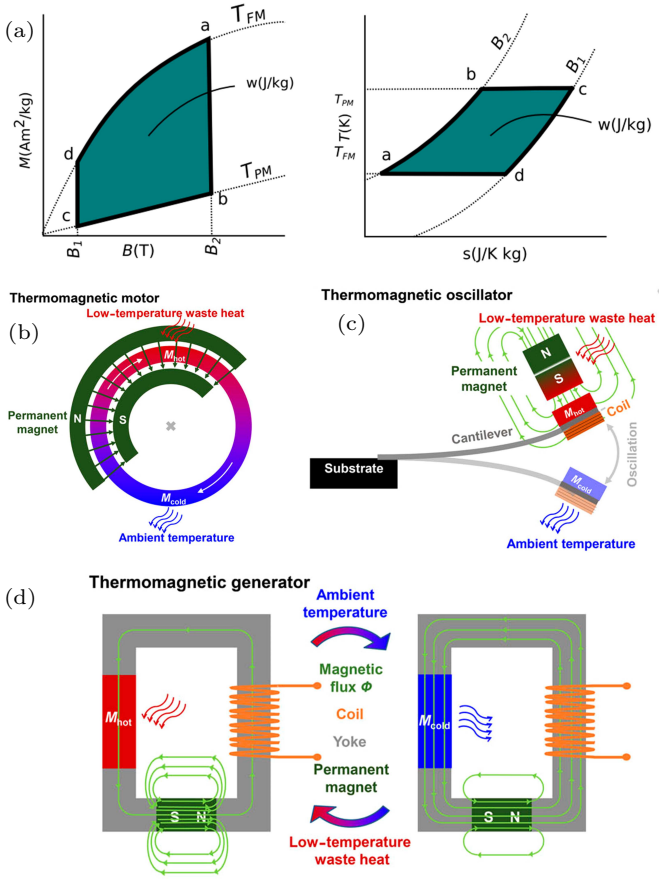


Fig. 3. (a) A work cycle for the TME cycle. (left) *M*–*B* diagram; (right) *s*–*T* diagram. Reproduced with permission.[112] Copyright 2014, Elsevier. (b) A rotatable ring of TMMs in a thermomagnetic motor. (c) Work flow of the thermomagnetic oscillator. (d) A working cycle in a static TMG. Reproduced under the terms of the CC BY license.[110] Copyright 2021, Authors.

In 2010, Srivastava *et al.* reported the first micro-TMG device, utilizing $Ni_{45}Co_5Mn_{40}Sn_{10}$ material in a single-circuit configuration, though with a low device efficiency of approximately 0.004% (Fig. 4(a)).[128] A proof-of-concept static TMG based on $(Mn,Fe)_2(P,As)$ material was later demonstrated in 2014 by Christiaanse and Brück.[112] To widen the operational temperature span, their design employed 48 disks of TMMs with graded T_C (300 K, 304 K, 307 K, 310 K) in a magnetic field generated by a NdFeB magnet. An optimized two-circuit magnetic topology was used to minimize stray fields (Fig. 4(b)), achieving a maximum average output power of about 0.048 mW. In 2018, Waske *et al.* designed a TMG demonstrator using La–Fe–Co–Si that significantly enhanced performance metrics, such as induced voltage, through a novel magnetic circuit topology (Fig. 4(c)).[15] Combined experimental and modeling results indicated this configuration effectively mitigated issues like magnetic stray fields, hysteresis, and complex TMM geometries; however, the maximum relative Carnot efficiency remained low (1.7×10^{-3}%). More recently, Liu *et al.* achieved a further performance boost without modifying the magnetic circuit, using Gd plates or $La(Fe,Si)_{13}H_y$/In composites to increase the induced average voltage from 0.04 V to 0.19 V.[129] Parallel efforts have focused on discovering new TMMs. For instance, Fries *et al.*[130] investigated the thermomagnetic properties of $Mn_{1-x}Co_xB$ and $Mn_{1-x}Fe_xB$ materials, where the MnB compound shows a high saturation magnetization $M =$ 156 Am^2·kg^{-1} and a sharp FM–PM phase transition (without hysteresis loss) at $T_C = 567$ K (tunable between 200–800 K). Chen *et al.*[125] compared various TMMs in a TMG device. Impressively, Zhang *et al.* reported that Ni–Mn–In based Heusler alloys with SOMT can be well suitable for TMGs with excellent performance,[131] and the thermal conductivity can

be significantly improved (65.2 $W \cdot m^{-1} \cdot K^{-1}$) in their Ni–Mn–In/In composite.[132] Furthermore, Dzekan *et al.* compiled a TMM library to evaluate efficiency and cost-effectiveness for use in thermomagnetic motors, oscillators, and generators, concluding that the best-performing TMMs can compete with thermoelectric materials for temperature gradients up to several tens of kelvins.[110] Despite these advances, TMG technology still faces significant challenges, including low power density, low conversion efficiency, and a limited portfolio of candidate materials covering the low-grade waste-heat temperature window. Nonetheless, ongoing progress in magnetic materials, system design, and optimization techniques indicates a promising pathway for future development.

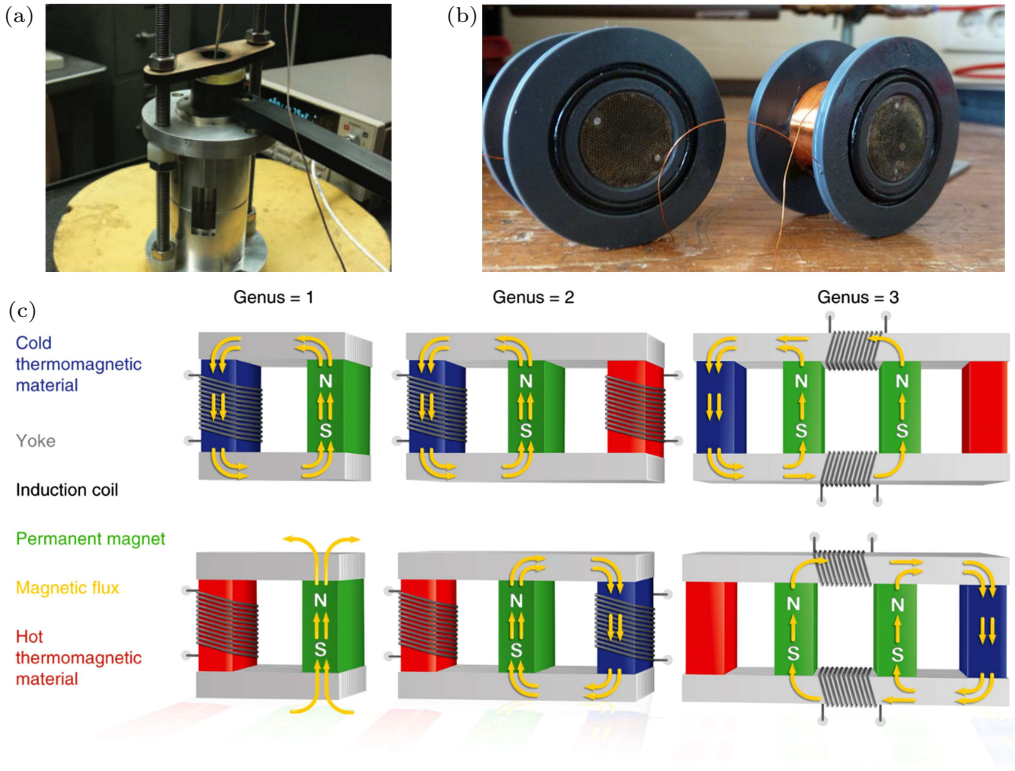


Fig. 4. (a) First TMG demonstrator with an unoptimized magnetic circuit.[128] Reproduced under the terms of the CC BY license. Copyright 2010, Authors. (b) An optimized topology with two magnetic circuits avoids magnetic stray fields.[112] Copyright 2014, Elsevier. (c) An optimized topology with three magnetic circuits.[111] Reproduced with permission. Copyright 2019, Springer Nature.

2.3. Micro- and nano-scale applications

The MCMs at lower dimensions such as the nanoscale are also promising in fields like micro-refrigerators, thermal switches, microfluidic pumps, energy harvesting devices, and biomedical applications.[133,134] For example, (i) micro-refrigerators: micro-scale magnetocaloric refrigerators are promising for on-chip cooling, sensors, and miniature electronic devices, with several designs already explored in simulation studies.[135] For instance, Kim *et al.* fabricated a micromachined magnetocaloric cooler by patterning silicon microfluidic channels, demonstrating operation under a 1.2 T magnetic field.[136] (ii) Magnetic hyperthermia: the MCE also enables medical applications such as controlled drug release and magnetic hyperthermia. Li *et al.* developed a magnetothermally responsive nanocarrier based on $Mn_{0.2}Zn_{0.8}Fe_2O_4$ nanoparticles that releases drugs under an alternating magnetic field.[137] FeRh alloys exhibiting a FOMT have been shown to act as switchable, high-contrast agents for magnetic resonance imaging (MRI) in a DC magnetic field.[138–140] Takhsha *et al.* reported that Ni–Mn–Ga epitaxial thin films promote the adhesion and proliferation of human fibroblasts without cytotoxicity, indicating their potential for biomedical interfaces.[59] Mn–Fe–P–Si particles have been applied for self-limiting biomedical thermal regulation.[141]

3. Typical MCMs for applications

In the past two decades, numerous FOMT and strong SOMT MCMs with GMCE have sprung up, including $Gd_5(Si_2Ge_2)$,[10] $(Mn,Fe)_2(P,X)$-based compounds (X = As, Ge, Si),[11] $La(Fe,Si)_{13}$-based materials,[12,34] NiMn-X based magnetic Heusler compounds (X = Ga, In, Sn, Sb)[35] with all-d-metal NiCoMnTi as a special case,[142] FeRh,[143] Mn_2Sb based alloys,[144] Mn–M–X (M = Co, Ni, and X = Si, Ge) alloys[37,38] and magnetocaloric high-entropy alloys (MHEAs).[145] These materials have strong coupling in the form of magnetoelastic (ME) or magnetostructural (MS) coupling, the mechanisms of which can be found elsewhere.[21,146] Advances related to typical ME coupled ma-

terials (including $(Mn,Fe)_2(P,Si)$-based and $La(Fe,Si)_{13}$-based compounds), MS coupled materials (including NiMn-based magnetic Heusler), and MHEAs are introduced below.

3.1. $(Mn,Fe)_2(P,Si)$ based compounds

The Fe_2P prototype compound, a strongly anisotropic hexagonal ferromagnet (space group P-62m),[147] undergoes a FOMT near $T_C \sim 216$ K.[148,149] Early studies of the quaternary derivative $(Mn,Fe)_2(P,As)$ by Fruchart and co-workers examined its magnetic and structural properties,[150,151] but the GMCE in this system was first reported by Brück *et al.* in 2000.[11] For the $(Mn,Fe)_2(P_{0.45}As_{0.55})$ compound, a FOMT was found at about 300 K with a large $|\Delta s_m|$ of 14.5 and 18.0 J·kg^{-1}·K^{-1} for $\Delta\mu_0 H$ of 2 T and 5 T, respectively.[11] In pursuit of non-toxic alternatives, the second-generation $(Mn,Fe)_2(P,Ge)$ and third-generation $(Mn,Fe)_2(P,Si)$ alloys were developed in 2007 and 2008.[152,153] The GMCE performance was largely preserved upon replacing As with Ge or Si,[154,155] with detailed comparisons available in Ref. [156]. This material family offers several advantages: excellent GMCE performance, absence of rare-earth and toxic elements, low cost, and tunable T_C and ΔT_{hys}. As illustrated in Fig. 5(a), the crystallographic site occupancies have been clearly determined. For example, Miao *et al.* confirmed that Mn atoms prefer the 3g site (in agreement with[157]) and that Fe atoms prefer the 3f site, while P/Si atoms randomly distribute on the 1b/2c sites (for the Si-rich case, Si atoms show a preference for the 2c site).[158] The origin of the GMCE has been attributed to a "mixed magnetism" mechanism, in which the Fe moments are quenched across the transition, as supported by density functional theory (DFT) calculations[159] and neutron diffraction (ND).[158,160] Synchrotron experiments further reveal a significant charge redistribution around Fe atoms during the ferromagnetic transition, resulting from competition between magnetism and covalent bonding.[161] Moreover, the c/a ratio is closely correlated with thermal hysteresis, which can be linked to transition-induced elastic strain energy.[162] Single crystals of $(Mn,Fe)_2(P,Si)$ have been successfully grown via the tin-flux method by Yibole *et al.*, revealing a preferred magnetization direction along the c-axis;[163] crystals with other compositions have also been obtained.[163–165] Miao *et al.* investigated the development of magnetic moments from spatial and temporal aspects in the PM regime of $(Mn,Fe)_2(P,Si)$ materials and studied the dynamics between short-range magnetic correlations and long-range magnetic ordering.[166] In certain compositions, a spin-density-wave (SDW) phase was observed to coexist with paramagnetic and ferromagnetic phases, and the SDW–ferromagnetic transition can be kinetically arrested at low temperatures.[167] In addition, the phase diagrams and the magnetic/structural properties of the $Mn_xFe_{2-x}P_{1-y}Si_y$ quaternary compounds have been reported.[159,168]

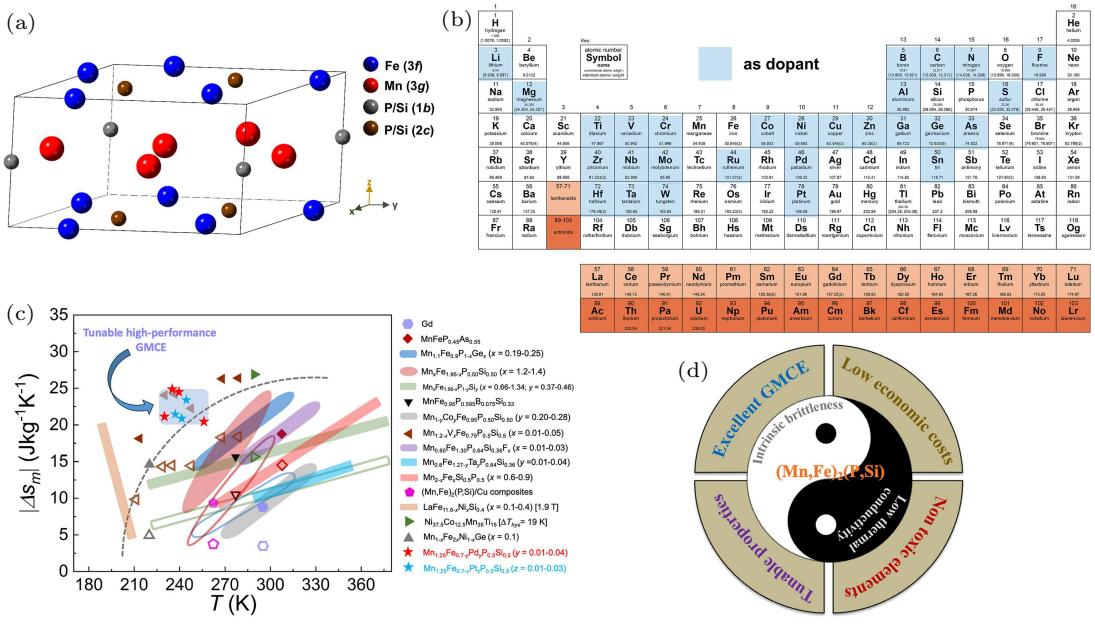


Fig. 5. (a). Crystal structure for the $(Mn,Fe)_2(P,Si)$ based MCMs.[193] Copyright 2022, F. Zhang. (b). Reported dopant for $(Mn,Fe)_2(P,Si)$ based MCMs so far. Copyright 2016, IUPAC. (c) Map of $|\Delta s_m|$ for $\Delta\mu_0 H = 1$ T (opensymbols) and 2 T (solid symbols).[185] Reproduced under the terms of the CC BY license. Copyright 2024, Authors. (d). Schematic figure related to advantages and disadvantages about $(Mn,Fe)_2(P,Si)$ based MCMs.[193] Reproduced under the terms of the CC BY license. Copyright 2022, F. Zhang.

Different optimization strategies for GMCE performance have been applied, e.g., chemical pressure engineering (substitutional/interstitial doping). Figure 5(b) lists the reported dopants for this family so far.[152,155,169–183] For example, it was found that B substitution can efficiently decrease the ΔT_{hys} from 75 K to only 1.6 K, and good reversibility was obtained after 10000 cycles ($\Delta T_{cyclic} \approx 2.8$ K with only $\Delta\mu_0 H$ of 1.1 T).[155] Similar hysteresis suppression has been

achieved with V, Nb, and Mo doping in $(Mn,Fe)_2(P,Si)$-based MCMs.[172,176,177,184] Independent control of T_C with minimal impact on hysteresis is another critical tuning strategy, where dopants mainly tune the T_C (towards a higher T_C by Li, B, C, Al, Ge, Zn, and Zr, and towards a lower T_C by N, F, S, V, Ni, Co, Cu, Ge, Nb, Mo, and Ru) but potentially also change the ΔT_{hys}. Notably, Zhang *et al.* demonstrated that W and Ta substitution can selectively adjust T_C while preserving or even enhancing GMCE without increasing ΔT_{hys}.[182,183] They also found that the 4d-Pd and 5d-Pt dopants for this family can well achieve a tunable $|\Delta s_m|$ in the range of 20–25 $J\cdot kg^{-1}\cdot K^{-1}$ ($\Delta\mu_0 H = 2$ T) with a low thermal hysteresis ΔT_{hys} (< 5.6 K). The performance surpasses almost all other $(Mn,Fe)_2(P,Si)$-based materials with ΔT_{hys} (< 10 K) reported until now (see Fig. 5(c)).[185] Interestingly, compared with B (low electronegativity), F, which possesses the highest electronegativity, can significantly improve the performance, increasing ΔT_{hys} and magnetic moments.[171] This contrast provides valuable insight into the role of electron behavior in this itinerant-electron metamagnet. In terms of material fabrication, Miao *et al.* successfully produced $(Mn,Fe)_2(P,Si)$-based magnetocaloric materials via 3D printing using selective laser melting (SLM).[186] Concurrently, machine learning has been employed for compositional optimization; Lai *et al.* developed a material with a T_C near 73 K, extending its applicability to the cryogenic range.[73] Similar data-driven approaches are being utilized to accelerate the design of $(Mn,Fe)_2(P,Si)$-based MCMs.[187] Addressing the common challenges of low thermal conductivity (λ) and intrinsic brittleness, a copper-composite strategy has been proposed (Fig. 5(d)).[188] Furthermore, Zhang *et al.*[133] synthesized $(Mn,Fe)_2(P,Si)$-based nanoparticles and systematically studied the influence of crystallite size and microstructure on the GMCE. This work may broaden the functional applications of such nanomaterials into areas like heterogeneous catalysis and secondary batteries.[189,190] Three reviews focused on $(Mn,Fe)_2(P,Si)$-based MCMs can be noted.[18,191,192]

3.2. $La(Fe,Si)_{13}$ based compounds

The binary compound $LaFe_{13-x}$ is thermodynamically unstable due to its positive heat of formation; however, the addition of silicon facilitates stabilization, yielding cubic $NaZn_{13}$-type $LaFe_{13-x}Si_x$ compounds (where $1.4 < x < 2.6$, space group Fm-$3c$). These materials undergo an isostructural FOMT. The crystal structure and atomic distribution are illustrated in Fig. 6(a).[194] Recent progress related to its MCE is summarized below.

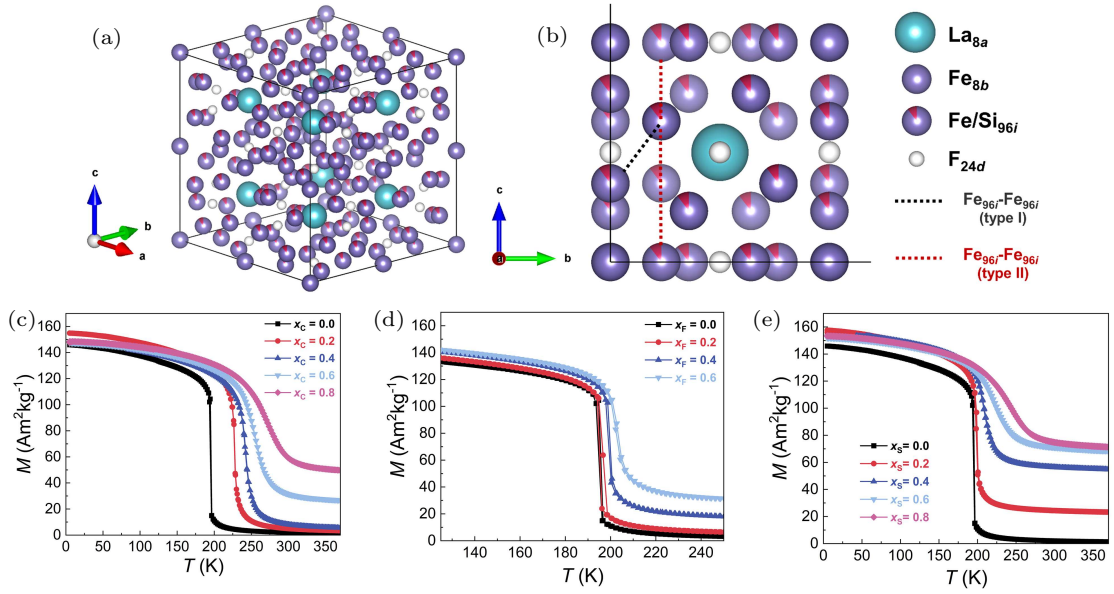


Fig. 6. (a) Schematic diagram of the atomic structure in one unit cell for the F-doped $La(Fe,Si)_{13}$ based compound. (b) Projection view from a direction in 1/8 part of one unit cell for the F-doped $La(Fe,Si)_{13}$ based compound.[194] (c)–(e) Iso-field M–T curves for different doped $LaFe_{11.6}Si_{1.4}$ samples in 1 T. Reproduced under the terms of the CC BY license. Copyright 2025, Authors.

Gruner *et al.*[195] observed significant changes in the element-resolved vibrational density of states (DOS) across the FOMT in $LaFe_{13-x}Si_x$, indicating that the transition stems from the itinerant electron metamagnetism of Fe atoms. Their findings suggest that lattice entropy, together with magnetic and electronic contributions, cooperatively enhances the total entropy change. Through x-ray absorption near-edge structure (XANES) spectroscopy, Shao *et al.*[196] provided evidence of electron transfer from hydrogen to Fe in $La(Fe,Si)_{13}H_x$ hydrides. Fujita[197] investigated hydrogen redistribution during the FOMT, revealing that annealing conditions influence hydrogen splitting behavior. Skokov *et al.*[198] examined the two-stage character of the FOMT in $LaFe_{11.8}Si_{1.2}$, offering atomistic-scale insights into the transition mechanism. A thermodynamic model was proposed to describe the dynamics of this two-step process by considering Gibbs free en-

ergy as a mixed state including chemical, elastic, and interfacial contributions.[199] Besides that, various optimization methods toward performance improvement have been developed. For example, magnetocaloric composites have been formed using composite materials with ductile second phases like epoxy resin,[200] Al,[201] Fe,[202,203] Cu,[204,205] Sn–In–Bi Field's metal,[206] In[207], Sn,[208] and Nb/Ta.[209] It was reported that the bending strength of the $LaFe_{11.6}Si_{1.4}$/Fe composite can reach up to 176 MPa using hot rolling.[203] Krautz *et al.* employed a core–shell architecture, fabricating composite wires consisting of a magnetocaloric core within a seamless austenitic steel jacket.[210,211] These thin wires can be assembled into various geometries. The process can also incorporate other ductile cladding materials, such as copper-based alloys or niobium, to further enhance thermal transport and corrosion resistance. Furthermore, various dopants (light elements (H,[212] B,[213] C,[214] N,[215] F,[194] S[194]), Cr,[216] Mn,[72] Co,[217] Ni,[218] Ce,[219] Pr,[220] Nd,[220] Gd[221]) have been introduced and function well in the $LaFe_{13-x}Si_x$ system. For example, in Fig. 6(b), Zhang *et al.* found that C, F, and S dopants increase T_C but with a negligible impact on ΔT_{hys} for the $LaFe_{11.6}Si_{1.4}$ compound, and the atomic distance of Fe_{96i}–Fe_{96i} (II) is key for the transition.[194] For the refined $(La_{1-x}Ce_x)_2Fe_{11}Si_2H_y$ alloys, the hysteresis losses can be reduced from 48.3 J·kg^{-1} to 0.6 J·kg^{-1}, and an excellent GMCE performance can be maintained after 10000 magnetic cycles ($\Delta T_{ad} = 2.03$ K for $\Delta\mu_0 H$ of 1.3 T).[219] Lai *et al.*[72] reduced the ΔT_{hys} (down to 1.5 K) by co-doping of Ce and Mn and moved the T_C into the cryogenic region (30–100 K). Two reviews related to the system can be found in Refs. [222,223]. Due to the iso-structural phase transition, the volume changes are around 0.3%, which offers excellent reversibility.[224] Together with Fe_2P-type MCMs, $La(Fe,Si)_{13}$-based compounds are the most promising alternatives for near-RT application under practical magnetic fields (< 2 T).[17]

3.3. Magnetic Heusler based alloys

Figure 7 highlights the diverse compositional space of potential X_2YZ-type Heusler alloys. In Ni/Mn-based magnetic Heusler compounds, magnetic ordering is strongly coupled to ferroelastic ordering through a structural (martensitic) phase transition — a feature absent in most non-martensitic Heusler alloys.[225] This pronounced MS coupling gives rise to novel functional properties, including giant magnetoresistance, large magnetostriction, the magnetic shape-memory effect, superelasticity, and the GMCE. Following the discovery of a reversible diffusionless FOMT in Ni–Mn–Ga compounds,[226,227] more smart materials with GMCE have been found in Ni–Mn–Ga,[228,229] Ni–Mn–In/Sb[230–232] and Ni–Mn–Sn-based[233] Heusler compounds. In Fig. 7(b), these compounds crystallize in $L2_1$ type fcc cubic structure (Fm-$3m$), and the $L2_1$ structure can transform to the low-temperature martensite with lower symmetry, such as tetragonal, orthorhombic, or monoclinic (L_{10}, 3(6)M, 5(10)M, and 7(14)M) types during the martensitic transformation.[234] The martensitic transition can be induced magnetically or thermally, driven by changes in Zeeman energy ($E_{Zeeman} = -\mu_0 \int MH\,dV$), as depicted in Fig. 7(c).[193] Enhanced reversibility is achieved by improving the geometric compatibility between austenite and martensite phases, which reduces transformation hysteresis.[235] Comprehensive reviews on conventional magnetic Heusler compounds are available elsewhere.[35,225,236–238] This section focuses instead on the unconventional all-d-metal Ni(Co)MnTi system, first reported in 2015,[142] with advantages such as a tunable T_C, RE-free composition (no main group elements), non-toxicity, and excellent mechanical properties.[239,240] Early studies on Ti stabilization and the lowering of the structural transition temperature provided important foundations.[241,242] Recent developments in these emerging all-d-metal Heusler compounds are reviewed in the following sections.

To optimize the microstructure, rapid-solidification techniques (e.g., melt-spinning, suction-casting and directional solidification) are applied.[244–250] For instance, $Ni_{37.5}Co_{12.5}Mn_{35}Ti_{15}$ ribbons show a $|\Delta s_m|$ as high as 27 J·kg^{-1}K^{-1} for a $\Delta\mu_0 H$ of 2 T.[246] The strong $\langle 001\rangle_A$ oriented polycrystalline $Ni_{36.6}Co_{12.8}Mn_{34.7}Ti_{15.9}$ alloy has $|\Delta s_m|$ of 23.2 J·kg^{-1}K^{-1} and 28.1 J·kg^{-1}·K^{-1} for $\Delta\mu_0 H$ of 5 T and 7 T, respectively, and shows an excellent mechanical performance with a maximum compressive strength of 2823 MPa and a strain of 17.7%.[249] In Fig. 7(d), by suction casting (SC), Zhang *et al.*[244] achieved a 67% $|\Delta s_m|$ improvement from 18.4 J·kg^{-1}·K^{-1} to 29.4 J·kg^{-1}·K^{-1} for a $\Delta\mu_0 H$ of 5 T, and a low ΔT_{hys} (5.5 K), therefore a very competitive reversible $|\Delta s_m|$ of 21.8 J·kg^{-1}·K^{-1} ($\Delta\mu_0 H = 5$ T). It is proposed that defect engineering can be applied to control the GMCE in these Heusler compounds.[244,251,252] Additionally, different annealing strategies have been applied.[253,254] Taubel *et al.*[254] found that the optimized heat treatment can significantly affect the magnetocaloric properties in $Ni_{35}Co_{15}Mn_{37}Ti_{13}$ with a $|\Delta s_m|$ of 20 J·kg^{-1}·K^{-1} and a ΔT_{ad} of -4 K for $\Delta\mu_0 H =$ 1.93 T. The preferred $B2$ disordering of austenite has been observed from ND experiments.[255] Moreover, different dopants like B,[256,257] V,[258] Cr,[259] Fe,[260–264] Cu,[265,266] Y[267] and Gd[268] can efficiently regulate its GMCE property. For example, introducing a small amount of interstitial boron into the $Ni_{36.5}Co_{13.5}Mn_{35}Ti_{15}$ compound effectively reduces the ΔT_{hys} (down to 4.4 K), while achieving a large reversible $|\Delta s_m|$ amounting to 18.9 J·kg^{-1}·K^{-1} at 283 K for $\Delta\mu_0 H =$ 5 T (22.0 J·kg^{-1}·K^{-1} for $\Delta\mu_0 H = 7$ T).[256] Similar beneficial effects of boron microalloying have also been reported in the ternary Ni–Mn–Ti system.[269–272] These ma-

terials have subsequently been tailored for cryogenic cooling applications.[74,273] Beckmann *et al.*[74] noted, however, that dissipation losses associated with the first-order transition and its hysteresis can limit cryogenic performance. Beyond MCE, all-d-metal Heusler compounds such as Ni(Co)MnTi also exhibit other functional properties, including a high-temperature shape-memory effect,[274] heterogeneous catalysis,[275] giant exchange bias,[276] TE application,[277] permanent magnets,[278] magnetoresistance,[266] and thermal energy storage applications.[51] Low-dimensional thin films of Ni(Co)MnTi materials have already been produced.[279,280] Beyond the experimental studies already reported,[258,281–285] high-throughput screening strategies have been successfully employed to accelerate the discovery of novel all-d-metal Heusler compounds,[277,278,286–289] and more interesting compounds are expected to be yielded in the near future.

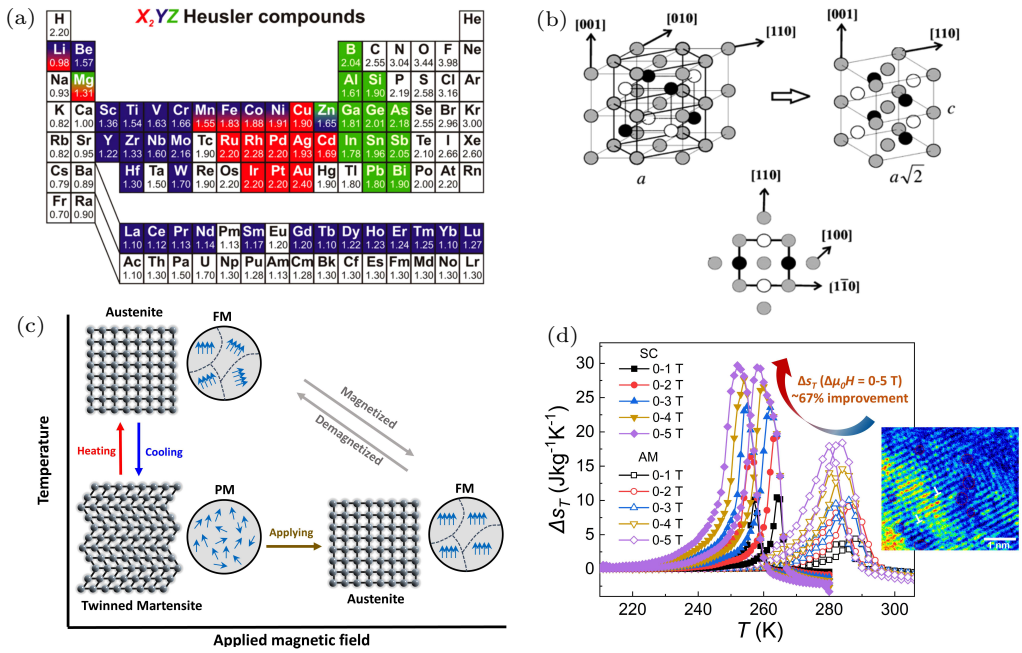


Fig. 7. (a) Periodic table of the elements showing different elements that can potentially form X_2YZ type Heusler compounds. Reproduced with permission.[243] Copyright 2011, Elsevier. (b) $L2_1$ austenite showing the relationship with the tetragonal unit cell (martensite) for the case of Ni_2MnGa from different directions.[35] Copyright 2009, IOP Publishing. (c). Schematic figures of the temperature- and magnetic field-induced martensitic transformation.[193] Reproduced under the terms of the CC BY license. Copyright 2022, F. Zhang. (d) Calculated Δs_m for SC and AM NiCoMnTi samples. The inset shows the defect distribution for AM sample.[244] Reproduced under the terms of the CC BY license. Copyright 2024, Authors.

3.4. Magnetocaloric high-entropy alloys

High-entropy alloys (HEAs) were initially conceived as single-phase solid-solution systems to explore the largely uncharted central regions of multicomponent phase diagrams.[290,291] To define HEAs, the equation for mixed configurational entropy $\Delta S_{\rm mix} = R\sum x_i \ln x_i$ is applied, where R is the gas constant and x_i is the mole fraction of the $i_{\rm th}$ element. As illustrated in Fig. 8(a), HEAs consist of five or more principal elements, each with a concentration between 5 and 35 at.% (composition-based criterion), and the $\Delta S_{\rm mix}$ should be high enough (entropy-based definition), e.g., $\Delta S_{\rm mix} \geq 1.5R$ (a compromise definition)[145] or $\Delta S_{\rm mix} > 1.61R$.[292] More details can be found in Refs. [293–295]. Crucially, magnetocaloric HEAs (McHEAs) must retain a single-phase solid-solution structure. Compared with conventional MCMs, McHEAs present several distinct advantages (Fig. 8(b)), e.g., (i) Cost and critical-element reduction — they lower material costs and mitigate over-reliance on scarce RE elements. (ii) Unique magnetic properties due to their complex microstructures and high $\Delta S_{\rm mix}$. (iii) Vast compositional space — the incorporation of multiple components offers a nearly limitless palette for fine-tuning properties, including the magnetocaloric response. (iv) McHEAs with SOMT always exhibit an MCE over a wide temperature range. This combination of versatility and tunability makes them promising new candidates for the development of both solid-state MCE and TME applications.

Since their emergence in 2013, numerous McHEAs have been developed (see Fig. 8(b)), evolving from initial equiatomic compositions[296] to non-equiatomic designs and, more recently, to systems exhibiting a FOMT.[145,297] For McHEAs without RE, for instance, Lucas *et al.*[298] studied the MCE in equiatomic FeCoNiCr McHEAs in 2013. Although the material showed moderate magnetocaloric properties ($|\Delta s_{\rm m}| < 0.4$ J·kg^{-1}·K^{-1} for $\Delta\mu_0 H = 2$ T), the tunable $T_{\rm C}$ and remarkable ductility have attracted considerable attention from the MCE community. Perrin *et al.*[299,300] attributed the modest MCE in such alloys to distributed exchange interactions resulting from compositional disorder; these interactions can be partially mitigated by Pd doping, which enhances both $T_{\rm C}$ and magnetocaloric performance.[301] Moreover, it was

reported that a $Fe_{25}Co_{25}Ni_{25}(Mo_{0.2}P_{0.4}B_{0.4})_{25}$ bulk metallic glass (BMG) can show a maximum $|\Delta s_m| = 0.98$ J·kg^{-1}·K^{-1} for $\Delta\mu_0 H = 2$ T around 560 K.[302] FeCoNiCuAlCr thin films were produced and exhibited a moderate MCE ($|\Delta s_m| = 0.53$ J·kg^{-1}·K^{-1} for $\Delta\mu_0 H = 5$ T) near RT.[303] For equiatomic McHEAs with RE, it was found that $Gd_{20}Tb_{20}Dy_{20}Al_{20}M_{20}$ BMGs display a SOMT with a T_C between 45 K and 112 K, with a maximum $|\Delta s_m|$ of 9.43 J·kg^{-1}·K^{-1}, 7.25 J·kg^{-1}·K^{-1} and 5.96 J·kg^{-1}·K^{-1} in $\Delta\mu_0 H = 5$ T for M = Co, Ni and Fe, respectively.[304] $Tm_{20}Ho_{20}Er_{20}Al_{20}Co_{20}$ BMGs show a stronger MCE with a maximum $|\Delta s_m| = 15.0$ J·kg^{-1}K^{-1} under the same field.[305] Notably, rare-earth-based McHEAs processed into microwires[306,307] and ribbons[76,308–311] via melt-extraction techniques often surpass their bulk counterparts in magnetocaloric response, offering either larger entropy changes or broader operating temperature spans.

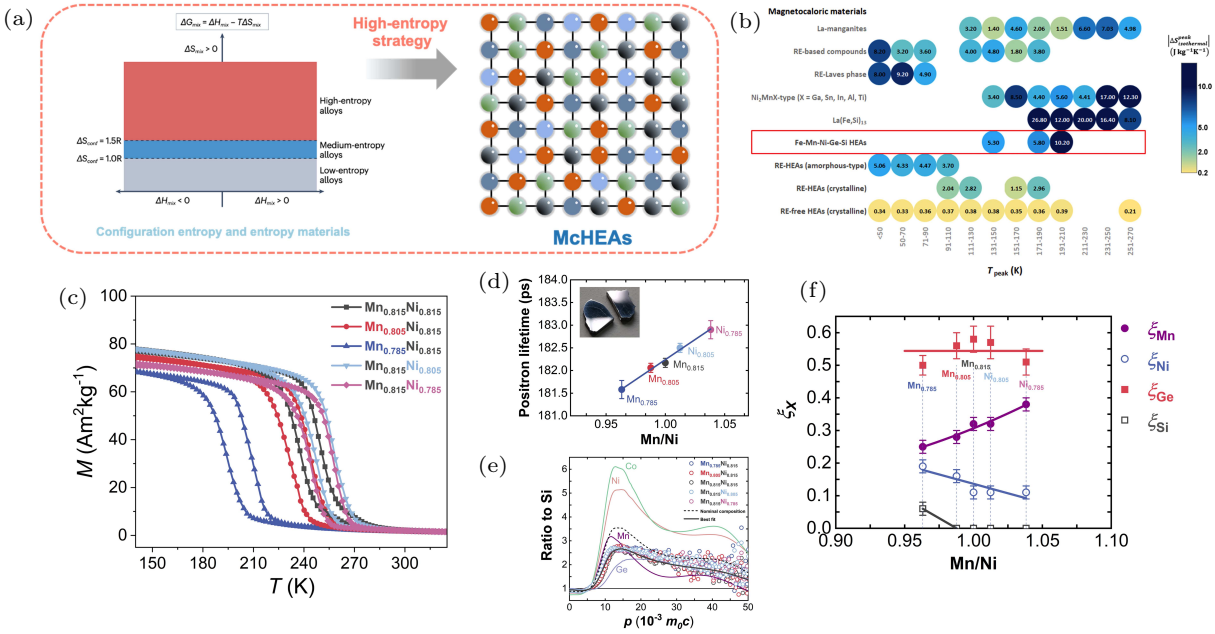


Fig. 8. (a) Definition of high entropy materials and McHEAs.[16] Copyright 2025, Elsevier. (b) MCE comparison matrix for McHEAs vs. conventional MCMs for 2 T.[297] Reproduced under the terms of the CC BY license. Copyright 2021, Authors. (c) M–T curves for different MnNiCoGeSi samples in a field of 1 T.[312] (d)–(f) Positron lifetime, ratio curves and fitting fractions for different samples, respectively.[312] Copyright 2025, Elsevier.

McHEAs with non-equiatomic compositions considerably extend the space of McHEAs. For example, the MCE was reported in non-equiatomic $Fe_{26.7}Ni_{26.7}Ga_{15.6}Mn_{20}Si_{11}$ and $Mn_{27}Cr_7Ni_{33}Ge_{25}Si_8$ HEAs, which show a maximum $|\Delta s_m|$ of 1.59 J·kg^{-1}·K^{-1} and 2.49 J·kg^{-1}·K^{-1}, respectively ($\Delta\mu_0 H = 2$ T).[313,314] Sarlar *et al.* concluded that the superior MCE performance of the $Mn_{27}Cr_7Ni_{33}Ge_{25}Si_8$ sample originates from a combination of the unconventional crystal structure and the constituent elements.[314] Zhang *et al.* synthesized $Al_{20}Mn_{20}Fe_{20}Co_{14.5+x}Cr_{25.5-x}$ McHEAs, reporting a moderate magnetocaloric performance.[315,316] Recently, $LaFe_{11}Si_2$-type materials have also been adapted into the McHEA paradigm by incorporating multiple transition metals (Co, Ni, Cr, Mn) on the Fe site.[317] Additionally, non-equiatomic McHEAs with RE always result in improved MCE performance because of the large moments of RE. For instance, $(Gd_{36}Tb_{20}Co_{20}Al_{20})_{100-x}Fe_x$ McHEAs exhibit a 25% wider working temperature span than their equiatomic counterparts, attributed to an amorphous/nanocrystalline dual-phase structure.[318] The working temperature span and $|\Delta s_m|$ can be further improved through DC current annealing,[319] compositional optimization[320] and hydrogenation treatment.[321] In perovskite-type systems,[322] $(Dy_{0.25}Ho_{0.25}Er_{0.25}Tb_{0.25})FeO_3$ and $(Gd_{0.2}Dy_{0.2}Ho_{0.2}Er_{0.2}Tb_{0.2})FeO_3$ exhibit a second-order spin-glass transition at low temperatures, induced by coexisting ferro- and antiferromagnetic coupling between disordered RE and Fe sublattices, yielding a considerable MCE over a broad temperature range for cryogenic applications.[323]

To overcome the inherently moderate magnetocaloric response of most McHEAs, a consequence of the compositional-disorder-broadened second-order transition, a property-directed strategy has recently been proposed to design McHEAs that retain a FOMT.[145,297] This approach transforms conventional FOMT-type MCMs into high-entropy variants through compositional diversification. For instance, for the $MM'X$-based MCMs, Law *et al.* developed the $Fe_{22.2}Mn_{22.3}Ni_{22.2}(Ge_xSi_{1-x})_{33.3}$ McHEAs with a GMCE ($|\Delta s_m|$ of 13 J·kg^{-1}·K^{-1} for $\Delta\mu_0 H = 2.5$ T),[324,325] effectively bridging the performance gap between conventional high-performance MCMs and earlier McHEAs (Fig. 8(b)). Subsequently, $(MnNiSi)_{1-x}(FeCoGe)_x$ and $Mn_{1.75}Fe_{0.25}CoNiGe_{1.6}Si_{0.4}$ McHEAs were produced by different authors, and both works present excellent GMCE properties, e.g., $|\Delta s_m| = 48.5$ J·kg^{-1}·K^{-1} for $\Delta\mu_0 H = 5$ T[326]

and low ΔT_{hys} (4.3 K).[327] Beyond composition, atomic-scale defect engineering offers an additional tuning strategy. As illustrated in Figs. 8(c)–8(f), Zhang *et al.* demonstrated that specific atomic vacancies (e.g., Mn or Ni vacancies) can effectively tailor the magnetocaloric properties of Mn–Co–Ni–Ge–Si-based McHEAs by modifying the local microstructure.[312] Through advanced characterization techniques, including synchrotron x-ray diffraction, *in-situ* neutron diffraction, HAADF-STEM, and positron annihilation spectroscopy, the underlying mechanism and the specific role of these vacancies have been elucidated.[312]

4. Opportunities, challenges, and perspective

Currently known MCMs are mainly found through low-efficiency trial-and-error experiments that typically heavily rely on empirical structure–property relationships, which always require a significant investment of time and resources.[328] High-throughput computational screening based on DFT calculations has been successfully employed to provide relatively accurate and time-efficient predictions of new MCMs and their magnetic properties.[328–331] In parallel, machine learning (ML) and deep learning (DL) techniques are increasingly being applied to accelerate the discovery of functional materials,[332] including in the field of magnetocaloric energy conversion.[333] These approaches have already facilitated the identification of new magnetocaloric compositions[73,187,334–337] and the optimization of prototype designs.[338–340] The effectiveness of ML, however, relies heavily on the availability of large, high-quality experimental datasets, underscoring the need for comprehensive and well-curated material databases. Advanced manufacturing methods, particularly additive manufacturing (AM), have also shown considerable progress in recent years. By using digital designs to consolidate feedstock materials layer-by-layer, AM enables the fabrication of complex 3D structures with minimal material waste and time.[341] This technology can help address long-standing challenges in MCMs, such as brittleness and phase inhomogeneity, through precise microstructural control achieved by rapid solidification in localized regions.[342] Recent efforts aimed at overcoming property "trade-off", for example, between magnetic performance, thermal conductivity, and mechanical strength, are increasingly focusing on microstructural engineering.[188,343,344] Furthermore, thin-film forms of MCMs are gaining attention for flexible and low-dimensional applications, including thermal management in advanced microelectronics. But interfacial thermal resistance, heat spreading, and cycling frequency limits should be regarded as key engineering considerations for these thin-film MCMs. The integration of intelligent computation, with its advantages of lower cost, speed, and precision, and advanced manufacturing for microstructural tailoring,[345] promises to accelerate the topological optimization and discovery of MCMs. However, several key challenges must be addressed to expedite development: (i) designing MCMs with improved MCE performance, (ii) developing suitable, low-cost permanent magnets (preferably RE-free or light-RE based) to generate strong magnetic fields, and (iii) optimizing system design and manufacturing costs. Material considerations such as reversibility, availability, criticality, and corrosion resistance should be prioritized. Beyond material development, the design and integration of MCMs into efficient devices also present a distinct set of challenges. For example, for the device-level engineering: (i) magnetic circuit design: the challenge of designing cost-effective, high-field permanent magnet arrays (the heaviest and most expensive part of an MR device)[17] using rare-earth-free or light-rare-earth magnets and optimized assemblies[346] should be emphasized. For TMG devices, it is crucial to optimize the magnetic circuit (e.g., optimized multi-circuit topologies) to minimize stray fields and maximize the useful magnetic field acting on the materials, directly impacting device power and efficiency. (ii) heat-exchange architecture: the integration of MCMs into porous beds or layered structures and the resulting trade-off between flow resistance, porosity, and heat transfer efficiency is a central practical problem. MCM/composite strategies can enhance thermal conductivity, and micro-channel designs can improve heat transfer and decrease the pressure drop. For long-term reliability and cyclic stability: (i) fatigue and mechanical degradation: the inherent brittleness of many intermetallic MCMs is a key challenge. Composite fabrication like core–shell wires, hot-rolled composites, and 3D-printed structures could be promising to improve mechanical durability and prevent material fragmentation during cycling. (ii) performance metrics for stability: more metrics should be highlighted as mentioned elsewhere.[17] In addition, a high-performing MR prototype needs to integrate MCMs, magnets, drives, pumps, controls, transfer fluid, and heat sinks, along with scalability for different applications. For system-level integration and scalability, the high cooling power always leads to challenges in magnet size/cost and the need for efficient, high-flow-rate fluid circulation. Therefore, achieving high efficiency in prototypes requires perfect synchronization between the optimized magnetic sources (currently, below 1 T is feasible for permanent magnets), the fluid flow valves/pumps, and the external heat exchangers. Over the next decade, research in magnetocalories is poised to benefit from rapid advances in experimental characterization, progressive manufacturing technologies, and high-performance computation. It is expected that these converging developments will help bridge the gap between advanced material discovery and cutting-edge engineering, ultimately bringing magnetocaloric technologies closer to large-scale application.

Acknowledgements

This work was supported by the open research fund of CSNS (Grant Nos. KFKT2022B04 and KFKT2022A05). F.Q. Zhang and Y. Ren acknowledge financial support from City University of Hong Kong (Project No. 9610533). F.Q. Zhang and Y. Ren would like to express sincere appreciation to the Hong Kong SAR of China for supporting the research under the Global STEM Professorship, and to the Hong Kong Jockey Club for supporting the research under the JC STEM Lab of Energy and Materials Physics.

References

[1] Chu S and Majumdar A 2012 *Nature* **488** 294
[2] Chu S, Cui Y and Liu N 2017 *Nat. Mater.* **16** 16
[3] International Energy Agency 2018 *The Future of Cooling: Opportunities for energy-efficient air conditioning*
[4] Li J N, Torelló A, Kovacova V, Prah U, Aravindhan A, Granzow T, Usui T, Hirose S and Defay E 2023 *Science* **382** 801
[5] Lyubina J 2017 *J. Phys. D: Appl. Phys.* **50** 053002
[6] Commission E 2018 *EU 2050 long-term strategy*
[7] China's policies and actions to address climate change
[8] Gutfleisch O, Willard M A, Brück E, Chen C H, Sankar S G and Liu J P 2011 *Adv. Mater.* **23** 821
[9] Franco V, Blazquez J S, Ipus J J, Law J Y, Moreno-Ramirez L M and Conde A 2018 *Prog. Mater. Sci.* **93** 112
[10] Pecharsky V K and Gschneidner K A 1997 *Phys. Rev. Lett.* **78** 4494
[11] Tegus O, Brück E, Buschow K H J and de Boer F R 2002 *Nature* **415** 150
[12] Hu F X, Shen B G, Sun J R and Zhang X X 2000 *Chin. Phys.* **9** 550
[13] Johra H, Filonenko K, Heiselberg P, Veje C, Dall'Olio S, Engelbrecht K and Bahl C 2019 *Renew. Energy* **136** 115
[14] Gueltig M, Wendler F, Ossmer H, Ohtsuka M, Miki H, Takagi T and Kohl M 2017 *Adv. Energy Mater.* **7** 1601879
[15] Waske A, Dzekan D, Sellschopp K, Berger D, Stork A, Nielsch K and Fahler S 2019 *Nat. Energy* **4** 68
[16] Zhang F Q and Ren Y 2025 *Handbook of Magnetic Materials*, edited by Brück E (Elsevier) p. 45
[17] Gottschall T, Skokov K P, Fries M, Taubel A, Radulov I, Scheibel F, Benke D, Riegg S and Gutfleisch O 2019 *Adv. Energy Mater.* **9** 1901322
[18] Chaudhary V, Chen X and Ramanujan R V 2019 *Prog. Mater. Sci.* **100** 64
[19] Moya X, Kar-Narayan S and Mathur N D 2014 *Nat. Mater.* **13** 439
[20] Moya X and Mathur N D 2020 *Science* **370** 797
[21] Smith A, Bahl C R H, Bjork R, Engelbrecht K, Nielsen K K and Pryds N 2012 *Adv. Energy Mater.* **2** 1288
[22] Zhang F Q, Miao X F, van Dijk N, Brück E and Ren Y 2024 *Adv. Energy Mater.* **14** 2400369
[23] Kitanovski A 2020 *Adv. Energy Mater.* **10** 1903741
[24] Greco A, Aprea C, Maiorino A and Masselli C 2019 *Int. J. Refrig.* **100** 1
[25] Xiang J S, Zhang C D, Gao Y, Schmidt W, Schmalzl K, Wang C W, Li B, Xi N, Liu X Y, Jin H, Li G, Shen J, Chen Z Y, Qi Y, Wan Y, Jin W T, Li W, Sun P J and Su G 2024 *Nature* **625** 270
[26] Brown G V 1976 *J. Appl. Phys.* **47** 3673
[27] Rosenblum S S, Steyert W A and Pratt W P 1977 *A continuous magnetic refrigerator operating near room temperature*, Los Alamos National Lab
[28] Annaorazov M P, Asatryan K A, Myalikgulyev G, Nikitin S A, Tishin A M and Tyurin A L 1992 *Cryogenics* **32** 867
[29] Annaorazov M P, Nikitin S A, Tyurin A L, Asatrayan K A and Dovletov A K 1996 *J. Appl. Phys.* **79** 1689
[30] Guo Z B, Du Y W, Zhu J S, Huang H, Ding W P and Feng D 1997 *Phys. Rev. Lett.* **78** 1142
[31] Pecharsky V K 2016 *Nat. Mater.* **15** 1059
[32] Czernuszewicz A, Mudryk Y, Cui J, Griffith L, Johnson D D and Slaughter J 2025 *Adv. Mater. Technol.* e00545
[33] Smith A 2013 *Eur. Phys. J. H* **38** 507
[34] Hu F X, Shen B G, Sun J R, Cheng Z H, Rao G H and Zhang X X 2001 *Appl. Phys. Lett.* **78** 3675
[35] Planes A, Manosa L and Acet M 2009 *J. Phys.: Condens. Matter* **21** 233201
[36] Liu J, Gottschall T, Skokov K P, Moore J D and Gutfleisch O 2012 *Nat. Mater.* **11** 620
[37] Trung N T, Zhang L, Caron L, Buschow K H J and Brück E 2010 *Appl. Phys. Lett.* **96** 172504
[38] Liu E K, Wang W H, Feng L, Zhu W, Li G J, Chen J L, Zhang H W, Wu G H, Jiang C B, Xu H B and de Boer F 2012 *Nat. Commun.* **3** 873
[39] Manosa L and Planes A 2017 *Adv. Mater.* **29** 1603607
[40] Zhang Y K, Wu J H, He J, Wang K and Yu G X 2021 *Renew. Sustain. Energy Rev.* **143** 110933
[41] Not Your Average Fridge Magnet: These High-Tech Magnets Will Keep Your Butter (and Beer) Cold
[42] Premiere of Cutting-Edge Cooling Appliance at CES 2015
[43] Magnetic fridge eliminates gases drastically reduces energy use
[44] Lionte S, Risser M and Muller C 2021 *Int. J. Refrig.* **122** 256
[45] Nakashima A T D, Fortkamp F P, de Sá N M, dos Santos V M A, Hoffmann G, Peixer G F, Dutra S L, Ribeiro M C, Lozano J A and Barbosa J R 2021 *Int. J. Refrig.* **122** 110
[46] Peixer G F, Silva M C R, Lorenzoni A, Hoffmann G, dos Santos D, do Rosario G M, Pagnan E, Teza H F, Silva P M, Dutra S L, Ribeiro M C, Rosa M A A, Dorng A, Vieira B P, Nakashima A T D, Wendhausen P A P, Teixeira C S, Lozano J A and Barbosa J R 2023 *Int. J. Refrig.* **151** 1
[47] Liang J R, Pickett J, Hermann S, Sittig T, Reichert T, Lehmann M, Stotzer J, Zwick J P, Greifenstein M, Strauch M, Skokov K, Gutfleisch O, Gottschall T, Fries M and Benke D 2026 *Appl. Therm. Eng.* **284** 129144
[48] Yu B F, Liu M, Egolf P W and Kitanovski A 2010 *Int. J. Refrig.* **33** 1029
[49] Usman A, Xiong F, Aftab W, Qin M L and Zou R Q 2022 *Adv. Mater.* **34** 2202457
[50] Freeman T B, Foster K E O, Troxler C J, Irvin C W, Aday A, Boetcher S K S, Mahvi A, Smith M K and Odukomaiya A 2023 *Adv. Energy Mater.* **13** 2204208
[51] Li S W, He L H, Lu H L, Hao J Z, Wang D K, Shen F R, Song C, Liu G J, Du P F, Wang Y D and Cong D Y 2023 *Acta Mater.* **249** 118852
[52] Sharar D J, Donovan B F, Warzoha R J, Wilson A A, Leff A C and Hanrahan B M 2019 *Appl. Phys. Lett.* **114** 143902
[53] Dumont O, Frate G F, Pillai A, Lecompte S, De Paepe M and Lemort V 2020 *J. Energy Storage* **32** 101756
[54] Han H, Kan A, Jin Y, Xia P and Tang W 2012 China Patent CN202297193-U
[55] Arora S 2018 *J. Power Sources* **400** 621
[56] Cool BatMan 2022 M-ERA.NET
[57] Al-Nimr M, Haddad O and Al-Samamah L 2023 *Energy* **283** 129131
[58] Jung Y, Kim M, Kim T, Ahn J, Lee J W and Ko S H 2023 *Nano-Micro Lett.* **15** 160
[59] Takhsha M, Furlani F, Panseri S, Casoli F, Uhlir V and Albertini F 2023 *ACS Appl. Bio Mater.* **6** 5009
[60] Giauque W F and MacDougall D P 1933 *Phys. Rev.* **43** 768
[61] Brendeng E and Hetland J 2004 *State of the art in liquefaction technologies for natural gas* (Dordrecht: Springer Netherlands)
[62] Biswas A, Chouhan R K, Thayer A, Mudryk Y, Hlova I Z, Dolotko O and Pecharsky V K 2022 *Phys. Rev. Mater.* **6** 114406
[63] Liu W, Scheibel F, Gottschall T, Bykov E, Dirba I, Skokov K and Gutfleisch O 2021 *Appl. Phys. Lett.* **119** 022408
[64] Numazawa T, Kamiya K, Utaki T and Matsumoto K 2014 *Cryogenics* **62** 185
[65] Zhang H, Gimaev R, Kovalev B, Kamilov K, Zverev V and Tishin A 2019 *Physica B* **558** 65
[66] Terada N and Mamiya H 2021 *Nat. Commun.* **12** 1212
[67] Liu W, Bykov E, Taskaev S, Bogush M, Khoyaylo V, Fortunato N, Aubert A, Zhang H B, Gottschall T, Wosnitza J, Scheibel F, Skokov K and Gutfleisch O 2022 *Appl. Mater. Today* **29** 101624

[68] Guillou F, Pathak A K, Paudyal D, Mudryk Y, Wilhelm F, Rogalev A and Pecharsky V K 2018 *Nat. Commun.* **9** 2925
[69] Archipley C, Barclay J, Meinhardt K, Whyatt G, Thomsen E, Holladay J, Cui J, Anderson I and Wolf S 2022 *Cryogenics* **128** 103588
[70] Barclay J, Brooks K, Cui J, Holladay J, Meinhardt K, Polikarpov E and Thomsen E 2019 *Cryogenics* **100** 69
[71] Ansarinasab H, Fatimah M and Khojasteh-Salkuyeh Y 2023 *J. Energy Storage* **65** 107304
[72] Lai J W, Sepehri-Amin H, Tang X, Li J, Matsushita Y, Ohkubo T, Saito A T and Hono K 2021 *Acta Mater.* **220** 117286
[73] Lai J W, Bolyachkin A, Terada N, Dieb S, Tang X, Ohkubo T, Sepehri-Amin H and Hono K 2022 *Acta Mater.* **232** 117942
[74] Beckmann B, Koch D, Pfeuffer L, Gottschall T, Taubel A, Adabifiroozjaei E, Miroshkina O N, Riegg S, Niehoff T, Kani N A, Gruner M E, Molina-Luna L, Skokov K P and Gutfleisch O 2023 *Acta Mater.* **246** 118695
[75] Khan A N, Diaz-Garcia A, Moreno-Ramirez L M, Law J Y and Franco V 2024 *J. Alloys Compd.* **973** 172938
[76] Zhang Y K, Zhu J, Li S, Wang J and Ren Z M 2022 *J. Mater. Sci. Technol.* **102** 66
[77] Ma Z P, Dong X S, Zhang Z Q and Li L W 2021 *J. Mater. Sci. Technol.* **92** 138
[78] Lampen-Kelley P, Madhogaria R, Bingham N S, Phan M H, Monteiro P M S, Steinke N J, Ionescu A, Barnes C H W and Srikanth H 2021 *Phys. Rev. Mater.* **5** 094404
[79] He W W, Yin Y, Gong Q H, Evans R F L, Gutfleisch O, Xu B X, Yi M and Guo W L 2023 *Small* **19** 2300333
[80] Biswas A, Zarkevich N A, Pathak A K, Dolotko O, Hlova I Z, Smirnov A V, Mudryk Y, Johnson D D and Pecharsky V K 2020 *Phys. Rev. B* **101** 224402
[81] Niehoff T, Beckmann B, Skokov K, Herrero A, Oleaga A, Bykov E, Salazar Mejia C, StraBheim M, Gutfleisch O, Wosnitza J and Gottschall T 2025 *Adv. Funct. Mater.* **35** 2505704
[82] Biswas A, Del Rose T, Mudryk Y, Ribeiro P O, Alho B P, de Sousa V S R, Nobrega E P, von Ranke P J and Pecharsky V K 2022 *J. Alloys Compd.* **897** 163186
[83] Kumar S, Muhammad R, Kim S, Yi J W, Son K and Oh H 2024 *Adv. Funct. Mater.* **34** 2402513
[84] Romero-Muniz C, Law J Y, Revuelta-Losada J, Moreno-Ramirez L M and Franco V 2023 *Innovation Mater.* **1** 100045
[85] EU project, 2022 https://www.hylical.eu/
[86] Wang Z X, Doring A M, Vasylkiv O, Tang X, Skokov K P, Terada N, Ohkubo T, Gutfleisch O and Sepehri-Amin H 2025 *Acta Mater.* **296** 121227
[87] Terada N, Mamiya H, Saito H, Nakajima T, Yamamoto T D, Terashima K, Takeya H, Sakai O, Itoh S, Takano Y, Hase M and Kitazawa H 2023 *Commun. Mater.* **4** 13
[88] Levinsky J J B, Beckmann B, Gottschall T, Koch D, Ahmadi M, Gutfleisch O and Blake G R 2024 *Nat. Commun.* **15** 8559
[89] Nakagome H, Kuriyama T, Ogiwara H, Fujita T, Yazawa T and Hashimoto T 1986 *Advances in Cryogenic Engineering*, edited by Fast R W (Boston: Springer) p. 753
[90] Li L W, Xu P, Ye S K, Li Y, Liu G D, Huo D X and Yan M 2020 *Acta Mater.* **194** 354
[91] Silva R S, Gainza J, dos Santos C, Rodrigues E F S, Dejoie C, Huttel Y, Biskup N, Nemes N M, Ferreira N S, Alonso A, Rodrigues J E F S, Martinez J L and Alonso J A 2023 *Chem. Mater.* **35** 2439
[92] Wang D S, Zheng X Q, Xu J W, He L H, Gao Y W, Huang H, Wu H, Cao X Y, Liu D, Shen J X, Wang G Y, Zhang J Y, Wu Y F, Hu F X, Wang S G and Shen B G 2024 *Chem. Mater.* **36** 1707
[93] Zhang L B, Dong Q X, Bai J L, Liu Q Y, Cheng J W, Li C D, Liu P Y, Sun Y R, Huang Y, Ren Z A and Chen G F 2024 *Chin. Phys. B* **33** 067101
[94] Mo Z J, Jiang J X, Tian L, Xie H C, Li Y, Zheng X Q, Zhang L, Gao X Q, Li Z X, Liu G D, Li L W and Shen J 2025 *J. Am. Chem. Soc.* **147** 14684
[95] Li L W 2016 *Chin. Phys. B* **25** 037502
[96] Hepburn I D, Davenport I and Smith A 1995 *Space Sci. Rev.* **74** 215
[97] Kwon D, Bae J and Jeong S 2022 *Cryogenics* **122** 103421
[98] Shirron P, Wegel D and DiPirro M 2006 *AIP Conf. Proc.* **850** 1573
[99] Balli M, Mansouri S, Dimitrov D Z, Fournier P, Jandl S and Juang J Y 2020 *Phys. Rev. Mater.* **4** 114411
[100] Zhang Y K, Hao W X, Lin J L, Li H F and Li L W 2024 *Acta Mater.* **272** 119946
[101] Zhang Y K, Na Y Z, Hao W X, Gottschall T and Li L W 2024 *Adv. Funct. Mater.* **34** 2409061
[102] Chen Z H, Yu S L, Zhang G C, Wang C K, Gao J H, Zhang Y C, Zhao Y N, Li Z X, Shen J and Tu H 2024 *Cryogenics* **143** 103955
[103] Yao J W, Ren W J, Guo Q, Liu P, Guan Z Q, Bao C J, Zhang Z Q, Huang D, Zhang K, Wang Y X, Zhao D L, He J and Li B 2025 *Mater. Today Phys.* **55** 101762
[104] Xu Q F, Zhao P, Chen M T, Wu R T, Dai W, Long L S and Zheng L S 2025 *Adv. Mater.* **37** 2414226
[105] Xu Q F, Chen M T, Wu R T, Long L S and Zheng L S 2024 *J. Am. Chem. Soc.* **146** 20116
[106] Wang B J, Liu X Y, Hu F X, Wang J T, Xiang J S, Sun P J, Wang J, Sun J R, Zhao T Y, Mo Z J, Shen J, Chen Y Z, Huang Q Z and Shen B G 2024 *J. Am. Chem. Soc.* **146** 35016
[107] Guo Q, Ren W J, Liu P, Yao J W, Xiang J S, Zhang K, Wang Y X, Kumara L S R, Wang X L, Li W and Li B 2025 *J. Am. Chem. Soc.* **147** 34862
[108] Firth A, Zhang B and Yang A D 2019 *Appl. Energy* **235** 1314
[109] Enescu D and Virjoghe E O 2014 *Renew. Sustain. Energy Rev.* **38** 903
[110] Dzekan D, Waske A, Nielsch K and Fahler S 2021 *APL Mater.* **9** 011105
[111] Waske A, Dzekan D, Sellschopp K, Berger D, Stork A, Nielsch K and Fahler S 2019 *Nat. Energy* **4** 68
[112] Christiaanse T and Brück E 2014 *Metall. Mater. Trans. E* **1** 36
[113] Kaneko G H, Concejao W A S, Colman F C, Cocci A S, Alves C S, Pupim G C, Kubota G H, Oliveira V C and Trevizoli P V 2021 *Appl. Therm. Eng.* **186** 116472
[114] Hey J, Repaka M, Li T and Tan J L 2022 *Energies* **15** 6334
[115] Coray P S, Wymann D, Brunner R and Vida N 2015 *Delft Days on Magneto Calorics (DDMC)*
[116] Joseph J, Ohtsuka M, Miki H and Kohl M 2020 *Joule* **4** 2718
[117] Joseph J, Fontana E, Devillers T, Dempsey N M and Kohl M 2023 *Adv. Funct. Mater.* **33** 2301250
[118] Deepak K, Varma V B, Prasanna G and Ramanujan R V 2019 *Appl. Energy* **233–234** 312
[119] Deepak K, Pattanaik M S and Ramanujan R V 2019 *Appl. Energy* **256** 113917
[120] Chun J S, Song H C, Kang M G, Kang H B, Kishore R A and Priya S 2017 *Sci. Rep.* **7** 41383
[121] Rodrigues C, Pires A, Goncalves I, Silva D, Oliveira J, Pereira A and Ventura J 2022 *Adv. Funct. Mater.* **32** 2110288
[122] Kishore R A and Priya S 2018 *Renew. Sustain. Energy Rev.* **81** 33
[123] Liu X L, Zhang H, Chen H D, Ma Z H, Qiao K M, Xie L L, Ou Z Q, Wang J, Hu F X and Shen B G 2023 *Appl. Therm. Eng.* **221** 119827
[124] Fink L, Nielsch K and Fahler S 2023 *J. Alloys Compd.* **966** 171435
[125] Chen H D, Ma Z H, Liu X L, Qiao K M, Xie L L, Li Z X, Shen J, Dai W, Ou Z Q, Yibole H, Tegus O, Taskaev S V, Chu K, Long Y and Zhang H 2022 *Appl. Energy* **306** 117999
[126] Ahmim S, Almanza M, Loyau V, Mazaleyrat F, Pasko A, Parrain F and LoBue M 2021 *J. Magn. Magn. Mater.* **540** 168428
[127] Dzekan D, Diestel A, Berger D, Nielsch K and Fahler S 2021 *Sci. Technol. Adv. Mater.* **22** 643
[128] Srivastava V, Song Y T, Bhatti K and James R D 2011 *Adv. Energy Mater.* **1** 97
[129] Liu X L, Chen H D, Huang J Y, Qiao K M, Yu Z Y, Xie L L, Ramanujan R V, Hu F X, Chu K, Long Y and Zhang H 2023 *Nat. Commun.* **14** 4811
[130] Fries M, Gercsi Z, Ener S, Skokov K P and Gutfleisch O 2016 *Acta Mater.* **113** 213
[131] Chen H D, Liu X L, Liu Y, Xie L L, Yu Z Y, Qiao K M, Liu M Z, Hu F X, Shen B G, Ramanujan R V, Chu K and Zhang H 2024 *Mater. Horiz.* **11** 2603
[132] Chen H D, Liu M Z, Yu Z Y, Qiao K M, Naeem M Z, Liu J Y, Xie L L, Liu Y, Huang M F, Li Z X, Shen J, Hu F X, Shen B G and Zhang H 2025 *Adv. Mater.* **37** 2500544
[133] Zhang F Q, Taake C, Huang B W, You X M, Ojiyed H, Shen Q, Dugulan I, Caron L, van Dijk N and Brück E 2022 *Acta Mater.* **224** 117532
[134] Belo J H, Pires A L, Araújo J P and Pereira A M 2019 *J. Mater. Res.* **34** 134
[135] Silva D J, Bordalo B D, Pereira A M, Ventura J and Araújo J P 2012 *Appl. Energy* **93** 570

[136] Kim S, Ghirlanda S, Adams C, Bethala B, Sambandam S N and Bhansali S 2007 *Int. J. Energy Res.* **31** 717
[137] Li J B, Qu Y, Ren J, Yuan W Z and Shi D L 2012 *Nanotechnology* **23** 505706
[138] Barbic M, Dodd S J, Morris H D, Dilley N, Marcheschi B, Huston A, Harris T D and Koretsky A P 2019 *Magn. Reson. Med.* **81** 2238
[139] Barbic M, Dodd S J, ElBidweihy H, Dilley N R, Marcheschi B, Huston A L, Morris H D and Koretsky A P 2021 *Magn. Reson. Med.* **85** 506
[140] Dodd S J, Gudino N, Zadorozhnii O, Stano M, Hajducek J, Arregi J A, Morris H D, Uhli V, Barbic M and Koretsky A P 2025 *Sci. Rep.* **15** 2779
[141] Uliss P, Hanggai W, Kahler F, Aprea E, Jia Q, Gkouzioti V, Frimat J P, Brück E and Boutry C M 2025 *Adv. Sci.* **13** e09914
[142] Wei Z Y, Liu E K, Chen J H, Li Y, Liu G D, Luo H Z, Xi X K, Zhang H W, Wang W H and Wu G H 2015 *Appl. Phys. Lett.* **107** 022406
[143] Chirkova A, Skokov K P, Schultz L, Baranov N V, Gutfleisch O and Woodcock T G 2016 *Acta Mater.* **106** 15
[144] Murgatroyd P A E, Routledge K, Durdy S, Gaultois M W, Surta T W, Dyer M S, Claridge J B, Savvin S N, Pelloquin D, Hébert S and Alaria J 2021 *Adv. Funct. Mater.* **31** 2100108
[145] Law J Y and Franco V 2023 *J. Mater. Res.* **38** 37
[146] Scheibel F, Gottschall T, Taubel A, Fries M, Skokov K P, Terwey A, Keune W, Ollefs K, Wende H, Farle M, Acet M, Gutfleisch O and Gruner M E 2018 *Energy Technol.* **6** 1397
[147] Rundqvist S and Jellinek F 1959 *Acta Chem. Scand.* **13** 425
[148] Wappling R, Haggstrom L, Ericsson T, Devanarayanan S, Karlsson E, Carlsson B and Rundqvist S 1975 *J. Solid State Chem.* **13** 258
[149] Lundgren L, Tarmohamed G, Beckman O, Carlsson B and Rundqvist S 1978 *Phys. Scr.* **17** 39
[150] Zach R, Guillot M and Fruchart R 1990 *J. Magn. Magn. Mater.* **89** 221
[151] Bacmann M, Soubeyroux J L, Barrett R, Fruchart D, Zach R, Niziol S and Fruchart R 1994 *J. Magn. Magn. Mater.* **134** 59
[152] Thanh D T C, Brück E, Tegus O, Klaasse J C P and Buschow K H J 2007 *J. Magn. Magn. Mater.* **310** E1012
[153] Thanh D T C, Brück E, Trung N T, Klaasse J C P, Buschow K H J, Ou Z Q, Tegus O and Caron L 2008 *J. Appl. Phys.* **103** 07B318
[154] Trung N T, Ou Z Q, Gortenmulder T J, Tegus O, Buschow K H J and Brück E 2009 *Appl. Phys. Lett.* **94** 102513
[155] Guillou F, Porcari G, Yibole H, van Dijk N and Brück E 2014 *Adv. Mater.* **26** 2671
[156] Yibole H, Guillou F, Zhang L, van Dijk N H and Brück E 2014 *J. Phys. D: Appl. Phys.* **47** 075002
[157] Neish M J, Oxley M P, Guo J, Sales B C, Allen L J and Chisholm M F 2015 *Phys. Rev. Lett.* **114** 106101
[158] Miao X F, Caron L, Roy P, Dung N H, Zhang L, Kockelmann W A, de Groot R A, van Dijk N H and Brück E 2014 *Phys. Rev. B* **89** 174429
[159] Dung N H, Ou Z Q, Caron L, Zhang L, Thanh D T C, de Wijs G A, de Groot R A, Buschow K H J and Brück E 2011 *Adv. Energy Mater.* **1** 1215
[160] Dung N H, Zhang L, Ou Z Q, Zhao L, van Eijck L, Mulders A M, Avdeev M, Suard E, van Dijk N H and Brück E 2012 *Phys. Rev. B* **86** 045134
[161] Boeije M F J, Roy P, Guillou F, Yibole H, Miao X F, Caron L, Banerjee D, van Dijk N H, de Groot R A and Brück E 2016 *Chem. Mater.* **28** 4901
[162] Roy P, Torun E and de Groot R A 2016 *Phys. Rev. B* **93** 094110
[163] Yibole H, Guillou F, Huang Y K, Blake G R, Lefering A J E, van Dijk N H and Brück E 2015 *Appl. Phys. Lett.* **107** 162403
[164] Sales B C, Susner M A, Conner B S, Yan J Q and May A F 2015 *Phys. Rev. B* **92** 104429
[165] Bao L L, Meijuan W, Yibole H, Ou Z Q and Guillou F 2024 *J. Alloys Compd.* **970** 172612
[166] Miao X F, Caron L, Cedervall J, Gubbens P C M, de Réotier P D, Yaouanc A, Qian F, Wildes A R, Luetkens H, Amato A, van Dijk N H and Brück E 2016 *Phys. Rev. B* **94** 014426
[167] Miao X F, Mitsui Y, Dugulan A I, Caron L, Thang N V, Manuel P, Koyama K, Takahashi K, van Dijk N H and Brück E 2016 *Phys. Rev. B* **94** 094426
[168] You X M, Maschek M, van Dijk N H H and Brück E 2022 *Entropy* **24** 2
[169] Batashev I, de Wijs G A, van Dijk N H and Brück E 2021 *J. Magn. Magn. Mater.* **537** 168179
[170] Miao X F, Thang N V, Caron L, Yibole H, Smith R I, van Dijk N H and Brück E 2016 *Scr. Mater.* **124** 129
[171] Zhang F Q, Batashev I, Shen Q, Wu Z Y, Smith R I, de Wijs G A, van Dijk N and Brück E 2022 *Acta Mater.* **234** 118057
[172] Lai J W, Huang B W, Miao X F, Thang N V, You X M, Maschek M, van Eijck L, Zeng D C, van Dijk N and Brück E 2019 *J. Alloys Compd.* **803** 671
[173] Ou Z Q, Dung N H, Zhang L, Caron L, Torun E, van Dijk N H, Tegus O and Brück E 2018 *J. Alloys Compd.* **730** 392
[174] Miao X F 2019 China Patent CN110343934B
[175] Feng J T, Qian F J, Shi D N and Yang H 2019 *Appl. Phys.* **9** 358
[176] Hu S Y, Miao X F, Liu J, Ou Z Q, Cong M Q, Haschuluu O, Gong Y Y, Qian F J, You Y R, Zhang Y J, Xu F and Brück E 2019 *Intermetallics* **114** 106602
[177] Miao X F, Gong Y, Zhang F Q, You Y R, Caron L, Qian F J, Guo W H, Zhang Y J, Gong Y Y, Xu F, van Dijk N and Brück E 2022 *J. Mater. Sci. Technol.* **103** 165
[178] Wada H, Nakamura K, Katagiri K, Ohnishi T, Yamashita K and Matsushita A 2014 *Jpn. J. Appl. Phys.* **53** 063001
[179] Liu D M, Zhang H, Wang S B, Xiao W Q, Zhang Z L, Tian N, Liu C X, Yue M, Huang Q Z, Zhang J X and Lynn J W 2015 *J. Alloys Compd.* **633** 120
[180] Kim S, Shin H, Chu I, Lee K, Lee K H and Lee W 2022 *J. Alloys Compd.* **890** 161798
[181] Wlodarczyk P, Hawelek L, Kowalczyk M, Kaminska M, Zackiewicz P, Polak M, Hreczka M and Kolano-Burian A 2016 *Solid State Sci.* **56** 23
[182] Zhang F Q, Smits S, Kiecana A, Batashev I, Shen Q, van Dijk N and Brück E 2023 *J. Alloys Compd.* **933** 167802
[183] Zhang F Q, Batashev I, van Dijk N and Brück E 2023 *Scr. Mater.* **226** 115253
[184] Lai J W, You X M, Dugulan I, Huang B W, Liu J, Maschek M, van Eijck L, Dijk N and Brück E 2020 *J. Alloys Compd.* **821** 153451
[185] Zhang F Q, Feng P J, Kiecana A, Wu Z Y, Bai Z W, Li W J, Chen H C, Yin W, Yan X W, Ma F J, Dijk N V, Brück E and Ren Y 2024 *Adv. Funct. Mater.* **34** 2409270
[186] Miao X F, Wang W Y, Liang H X, Qian F J, Cong M Q, Zhang Y J, Muhammad A, Tian Z J and Xu F 2020 *J. Mater. Sci.* **55** 6660
[187] Tu D F, Yan J Q, Xie Y B, Li J, Feng S, Xia M X, Li J G and Alex P L 2022 *J. Mater. Sci. Technol.* **96** 241
[188] Miao X F, Wang C X, Liao T W, Ju S H, Zha J J, Wang W Y, Liu J, Zhang Y J, Ren Q Y, Xu F and Caron L 2023 *Acta Mater.* **242** 118453
[189] Schipper D E, Zhao Z H, Thirumalai H, Leitner A P, Donaldson S L, Kumar A, Qin F, Wang Z M, Grabow L C, Bao J M and Whitmire K H 2018 *Chem. Mater.* **30** 3588
[190] Zhang Y, Zhang H J, Feng Y Y, Liu L and Wang Y 2015 *ACS Appl. Mater. Interfaces* **7** 26684
[191] Miao X F, Hu S Y, Xu F and Brück E 2018 *Rare Met.* **37** 723
[192] Ho K Y, Zhang F Q, Miao X F, van Dijk N, Brück E and Ren Y 2025 *Metal. Mater.* **2** e70012
[193] Zhang F Q 2022 *Tuning giant magnetocaloric materials: A study of $(Mn,Fe)_2(P,Si)$ and NiCoMnTi Heusler compounds*, PhD thesis, (Delft University of Technology)
[194] Zhang F Q, Wu Z Y, Zhang X F, Chi X, Wu Z D, Gao J R, Chen H C, Yin W, Lienert U, Dippel A C, Zimmermann M V, van Dijk N, Brück E and Ren Y 2025 *Adv. Sci.* **12** 2416288
[195] Gruner M E, Keune W, Roldan Cuenya B, Weis C, Landers J, Makarov S I, Klar D, Hu M Y, Alp E E, Zhao J, Krautz M, Gutfleisch O and Wende H 2015 *Phys. Rev. Lett.* **114** 057202
[196] Shao Y Y, Lu B F, Zhang M X and Liu J 2018 *Acta Mater.* **150** 206
[197] Fujita A 2019 *Acta Mater.* **169** 162
[198] Skokov K P, Karpenkov A Y, Karpenkov D Y, Radulov I A, Günzing D, Eggert B, Rogalev A, Wilhelm F, Liu J, Shao Y, Ollefs K, Gruner M E, Wende H and Gutfleisch O 2023 *Appl. Phys. Rev.* **10** 031408
[199] Hardy V, Hamane R, Veillon F, Risser M and Guillou F 2022 *Acta Mater.* **231** 117869
[200] Zhang H, Sun Y J, Niu E, Hu F X, Sun J R and Shen B G 2014 *Appl. Phys. Lett.* **104** 062407
[201] Zhang M X, Ouyang Y, Zhang Y F and Liu J 2020 *J. Alloys Compd.* **823** 153846
[202] Shao Y Y, Liu Y F, Wang K, Zhang M X and Liu J 2020 *Acta Mater.* **195** 163
[203] Miao L Y, Lu X, Wei Z Y, Zhang Y F, Zhang Y X and Liu J 2023 *Acta Mater.* **245** 118635

[204] Lyubina J, Hannemann U, Cohen L F and Ryan M P 2012 *Adv. Energy Mater.* **2** 1323
[205] Liu J, Zhang M X, Shao Y Y and Yan A R 2015 *IEEE Trans. Magn.* **51** 2501502
[206] Radulov I A, Karpenkov D Y, Skokov K P, Karpenkov A Y, Braun T, Brabander V, Gottschall T, Pabst M, Stoll B and Gutfleisch O 2017 *Acta Mater.* **127** 389
[207] Wang Y X, Zhang H, Liu E K, Zhong X C, Tao K, Wu M L, Xing C F, Xiao Y N, Liu J and Long Y 2018 *Adv. Electron. Mater.* **4** 1700636
[208] Zhang H, Liu J, Zhang M X, Shao Y Y, Li Y and Yan A 2016 *Scr. Mater.* **120** 58
[209] Lu C X, Wu Q M, Wang H F, Wang X J and Li L W 2021 *J. Alloys Compd.* **872** 159553
[210] Funk A, Freudenberger J, Waske A and Krautz M 2018 *Mater. Today Energy* **9** 223
[211] Krautz M, Beyer L, Funk A, Waske A, Weise B, Freudenberger J and Gottschall T 2020 *Mater. Des.* **193** 108832
[212] Fujita A, Fujieda S, Fukamichi K, Yamazaki Y and Iijima Y 2002 *Mater. Trans.* **43** 1202
[213] Xie S H, Li J Q and Zhuang Y H 2007 *J. Magn. Magn. Mater.* **311** 589
[214] Chen Y F, Wang F, Shen B G, Wang G J and Sun J R 2003 *J. Appl. Phys.* **93** 1323
[215] Balli M, Rosca M, Fruchart D and Gignoux D 2009 *J. Magn. Magn. Mater.* **321** 123
[216] Moreno-Ramirez L M, Romero-Muniz C, Law J Y, Franco V, Conde A, Radulov I A, Maccari F, Skokov K P and Gutfleisch O 2019 *Acta Mater.* **175** 406
[217] Hao J Z, Hu F X, Wang J T, Shen F R, Yu Z B, Zhou H B, Wu H, Huang Q Z, Qiao K M, Wang J, He J, He L H, Sun J R and Shen B G 2020 *Chem. Mater.* **32** 1807
[218] Moreno-Ramirez L M, Romero-Muniz C, Law J Y, Franco V, Conde A, Radulov I A, Maccari F, Skokov K P and Gutfleisch O 2018 *Acta Mater.* **160** 137
[219] Liu Y F, Fu X Q, Yu Q, Zhang M X and Liu J 2021 *Acta Mater.* **207** 116687
[220] Davarpanah A, Radulov I, Shayanfar N, Maccari F, Skokov K, Amaral J and Gutfleisch O 2021 *J. Phys. D: Appl. Phys.* **54** 225001
[221] Yan Y J, Liu C S, Lu W C, Sun Y, Zhu W T, Nie X L, Sang X H, Zhao W Y and Zhang Q J 2022 *J. Alloys Compd.* **910** 164858
[222] Paul-Boncour V and Bessais L 2021 *Magnetochemistry* **7** 13
[223] Shao Y Y, Miao X F, Zhang Y J, Xu F and Liu J 2022 *J. Magn. Magn. Mater.* **564** 170057
[224] Pulko B, Tusek J, Moore J D, Weise B, Skokov K, Mityashkin O, Kitanovski A, Favero C, Fajfar P, Gutfleisch O, Waske A and Foredos A 2015 *J. Magn. Magn. Mater.* **375** 65
[225] Tavares S, Yang K S and Meyers M A 2023 *Prog. Mater. Sci.* **132** 101017
[226] Zasimchuk I K, Kokorin V V, Martynov V V, Tkachenko A V and Cherennko V A 1990 *Phys. Met. Metallogr.* **69** 104
[227] Ullakko K, Huang J K, Kantner C, OHandley R C and Kokorin V V 1996 *Appl. Phys. Lett.* **69** 1966
[228] Hu F X, Shen B G and Sun J R 2000 *Appl. Phys. Lett.* **76** 3460
[229] Hu F X, Shen B G, Sun J R and Wu G H 2001 *Phys. Rev. B* **64** 132412
[230] Sutou Y, Imano Y, Koeda N, Omori T, Kainuma R, Ishida K and Oikawa K 2004 *Appl. Phys. Lett.* **85** 4358
[231] Kainuma R, Imano Y, Ito W, Sutou Y, Morito H, Okamoto S, Kitakami O, Oikawa K, Fujita A, Kanomata T and Ishida K 2006 *Nature* **439** 957
[232] Han Z D, Wang D H, Zhang C L, Tang S L, Gu B X and Du Y W 2006 *Appl. Phys. Lett.* **89** 182507
[233] Krenke T, Duman E, Acet M, Wassermann E F, Moya X, Manosa L and Planes A 2005 *Nat. Mater.* **4** 450
[234] Heczko O, Seiner H and Fahler S 2022 *MRS Bull.* **47** 618
[235] Bhattacharya K, Conti S, Zanzotto G and Zimmer J 2004 *Nature* **428** 55
[236] Felser C, Wollmann L, Chadov S, Fecher G H and Parkin S S P 2015 *APL Mater.* **3** 041518
[237] Felser C and Hirohata A 2016 *Heusler alloys properties, growth, applications* (Springer Nature)
[238] Rio-López N A, Lázpita P, Salazar D, Petrenko V I, Plazaola F, Cherenko V and Porro J M 2021 *Metals* **11** 829
[239] de Paula V G and Reis M S 2021 *Chem. Mater.* **33** 5483
[240] Bachagha T and Sunol J J 2023 *Metals* **13** 111
[241] Mater J 2009 *Sci. Technol.* **25** 649
[242] Belosludtseva E S, Kuranova N N, Kourov N I, Pushin V G and Uksusnikov A N 2015 *Tech. Phys.* **60** 1330
[243] Graf T, Felser C and Parkin S S P 2011 *Prog. Solid State Chem.* **39** 1
[244] Zhang F Q, Wu Z Y, Wang J L, Chen W Y, Wu Z D, Chi X, Zhao C L, Eijt S, Schut H, Bai X D, Ren Y, van Dijk N and Brück E 2024 *Acta Mater.* **234** 118057
[245] Ma C C, Liu K, Han X Q, Yang S, Ye N and Tang J C 2020 *J. Magn. Magn. Mater.* **493** 165733
[246] Bez H N, Pathak A K, Biswas A, Zarkevich N, Balema V, Mudryk Y, Johnson D D and Pecharsky V K 2019 *Acta Mater.* **173** 225
[247] Liu K, Han X Q, Yu K, Ma C C, Zhang Z S, Song Y, Ma S C, Zeng H, Chen C C, Luo X H, Rehman S U and Zhong Z C 2019 *Intermetallics* **110** 106472
[248] Liu K, Ma S C, Ma C C, Han X Q, Yu K, Yang S, Zhang Z S, Song Y, Luo X H, Chen C C, Rehman S U and Zhong Z C 2019 *J. Alloys Compd.* **790** 78
[249] Guan Z Q, Bai J, Sun S D, Gu J L, Liang X Z, Zhang Y D, Esling C, Zhao X and Zuo L 2022 *Appl. Mater. Today* **29** 101634
[250] Li Y, Qin L, Zhang H G and Li L W 2022 *Chin. Phys. B* **31** 087103
[251] Unzueta I, Sanchez-Alarcos V, Recarte V, Pérez-Landazabal J I, Zabala N, Garcia J A and Plazaola F 2019 *Phys. Rev. B* **99** 064108
[252] Unzueta I, de R-Lorente D A, Cesari E, Sanchez-Alarcos V, Recarte V, Pérez-Landazabal J I, Garcia J A and Plazaola F 2019 *Phys. Rev. Lett.* **122** 165701
[253] Zhang Y X, Zeng H, Yu G, Liu K, Ma S C, Yang K, Zhao X W, Yuan G, Luo X H, Chen C C and Zhong Z C 2020 *Intermetallics* **125** 106882
[254] Taubel A, Beckmann B, Pfeuffer L, Fortunato N, Scheibel F, Ener S, Gottschall T, Skokov K P, Zhang H B and Gutfleisch O 2020 *Acta Mater.* **201** 425
[255] Koch D, Beckmann B, Fortunato N M, Miroshkina O N, Gruner M E, Zhang H B, Gutfleisch O and Donner W 2022 *J. Appl. Phys.* **131** 073903
[256] Zhang F Q, Batashev I, van Dijk N and Brück E 2022 *Phys. Rev. Appl.* **17** 054032
[257] Guan Z Q, Bai J, Zhang Y, Gu J L, Morley N, Zhang Y D, Esling C, Zhao X and Zuo L 2023 *Mater. Today Phys.* **36** 101183
[258] Li Y, Ye X Y, Lou L J, Wang L F and Qin L 2023 *J. Supercond. Nov. Magn.* **36** 631
[259] Khan A N, Moreno-Ramírez L M, Diaz-Garcia A, Law J Y and Franco V 2023 *J. Alloys Compd.* **931** 167559
[260] Zeng Q Q, Shen J L, Zhang H N, Chen J, Ding B, Xi X K, Liu E K, Wang W H and Wu G H 2019 *J. Phys.: Condens. Matter* **31** 425401
[261] Liu S L, Xuan H C, Cao T, Wang L B, Xie Z G, Liang X H, Li H, Feng L, Chen F H and Han P D 2019 *Phys. Status Solidi A* **216** 1900563
[262] Li Y, Huang S Y, Wang W H, Liu E K and Li L W 2020 *J. Appl. Phys.* **127** 233907
[263] Li Y, Qin L, Huang S Y and Li L W 2022 *Sci. China Mater.* **65** 486
[264] Samanta S, Ghosh S, Chatterjee S and Mandal K 2022 *J. Alloys Compd.* **910** 164929
[265] Zhang F Q, Westra K, Shen Q, Batashev I, Kiecana A, van Dijk N and Brück E 2022 *J. Alloys Compd.* **906** 164337
[266] Samanta S, Chatterjee S, Sinha J and Mandal K 2023 *Phys. Rev. Mater.* **7** 084406
[267] Huang S Y, Qin L, Li Y and Li L W 2021 *Mater. Lett.* **302** 130376
[268] Xu F, Zhu C, Wang J, Luo F, Zhu X Q, Xu J H, Chen S Q, Wang J F, Ma G L, Chen F H, Kuang Y F, He J and Sun Z G 2023 *J. Alloys Compd.* **960** 170768
[269] Cong D Y, Xiong W X, Planes A, Ren Y, Manosa L, Cao P Y, Nie Z H, Sun X M, Yang Z, Hong X F and Wang Y D 2019 *Phys. Rev. Lett.* **122** 255703
[270] Aznar A, Gracia-Condal A, Planes A, Lloveras P, Barrio M, Tamarit J L, Xiong W X, Cong D Y, Popescu C and Manosa L 2019 *Phys. Rev. Mater.* **3** 044406
[271] Guan Z Q, Bai J, Zhang Y, Sun S D, Gu J L, Liang X Z, Zhang Y D, Esling C, Zhao X and Zuo L 2023 *J. Alloys Compd.* **930** 167477
[272] Guan Z Q, Bai J, Zhang Y, Gu J L, Zhang Y D, Esling C, Zhao X and Zuo L 2023 *Scr. Mater.* **229** 115353
[273] Guan Z Q, Bai J, Zhang Y, Gu J L, Liang X Z, Zhang Y D, Esling L D, Zhao X and Zuo L 2022 *J. Appl. Phys.* **131** 165107
[274] Li S H, Cong D Y, Xiong W X, Chen Z, Zhang X, Nie Z H, Li S W, Li R G, Wang Y K, Cao Y X, Ren Y and Wang Y D 2021 *ACS Appl. Mater. Interfaces* **13** 31870

[275] Jin T and Jung Y 2022 *Top. Catal.* **65** 208
[276] Samanta S, Ghosh S and Mandal K 2022 *J. Phys.: Condens. Matter* **34** 105801
[277] Tanzim M F, Fortunato N, Samthrakis I, Xie R W, Opahle I, Gutfleisch O and Zhang H B 2023 *Adv. Funct. Mater.* **33** 2214967
[278] Marathe M and Herper H C 2023 *Phys. Rev. B* **107** 174402
[279] Yu K, Liu K, Ma S C, Han X Q, Zhang Z S, Song Y, Zhang Y X, Chen C C, Luo X H and Zhong Z C 2019 *J. Magn. Magn. Mater.* **484** 31
[280] Ling Y C, Hu Y, Chi X D, Chen J W, Wang H B, Niu B, Wu D, Xu M X, Han Z D, Du J and Xu Q Y 2022 *J. Appl. Phys.* **131** 173902
[281] Peng L, Zhang Q Q, Wang N, Xia Z H, Zhang Y J, Wu Z G, Liu E K and Liu Z H 2023 *Chin. Phys. B* **32** 017102
[282] Dong J, Liu Z H, Si X D, Zhou T, Lin J and Liu Y S 2023 *Solid State Commun.* **362** 115099
[283] Tan J G, Liu Z H, Zhang Y J, Li G T, Zhang H G, Liu G D and Ma X Q 2019 *Results Phys.* **12** 1182
[284] Jacob G A and Joseyphus R J 2021 *Phys. Status Solidi A* **218** 2100050
[285] Zeng Q Q, Du Z W, Han X L, Wang B B, Wu G H and Liu E K 2024 *Acta Mater.* **262** 119429
[286] Sanvito S, Oses C, Xue J K, Tiwari A, Zic M, Archer T, Tozman P, Venkatesan M, Coey M and Curtarolo S 2017 *Sci. Adv.* **3** e1602241
[287] Han Y L, Wu M X, Feng Y, Cheng Z X, Lin T T, Yang T, Khenata R and Wang X T 2019 *IUCrJ* **6** 465
[288] Li G J, Xu L, Ding Z W and Cao Z H 2023 *Appl. Phys. Lett.* **123** 022401
[289] Li G J, Liu E K, Wang W H and Wu G H 2023 *Phys. Rev. B* **107** 134440
[290] Cantor B, Chang I T H, Knight P and Vincent A J B 2004 *Mater. Sci. Eng. A* **375–377** 213
[291] Yeh J W, Chen S K, Lin S J, Gan J Y, Chin T S, Shun T T, Tsau C H and Chang S Y 2004 *Adv. Eng. Mater.* **6** 299
[292] Miracle D B and Senkov O N 2017 *Acta Mater.* **122** 448
[293] George E P, Raabe D and Ritchie R O 2019 *Nat. Rev. Mater.* **4** 515
[294] Hsu W L, Tsai C W, Yeh A C and Yeh J W 2024 *Nat. Rev. Chem.* **8** 471
[295] Han L L, Zhu S Y, Rao Z Y, Scheu C, Ponge D, Ludwig A, Zhang H B, Gutfleisch O, Hahn H, Li Z M and Raabe D 2024 *Nat. Rev. Mater.* **9** 846
[296] Yu S L, Tian L, Wang J F, Zhao X G, Li D, Mo Z J and Li B 2024 *Chin. Phys. B* **33** 057502
[297] Law J Y and Franco V 2021 *APL Mater.* **9** 080702
[298] Lucas M S, Belyea D, Bauer C, Bryant N, Michel E, Turgut Z, Leontsev S O, Horwath J, Semiatin S L, McHenry M E and Miller C W 2013 *J. Appl. Phys.* **113** 17A923
[299] Perrin A, Sorescu M, Burton M T, Laughlin D E and McHenry M 2017 *JOM* **69** 2125
[300] Perrin A, Sorescu M, Ravi V, Laughlin D E and McHenry M E 2019 *AIP Adv.* **9** 035329
[301] Belyea D D, Lucas M S, Michel E, Horwath J and Miller C W 2015 *Sci. Rep.* **5** 15755
[302] Wu K N, Liu C, Li Q, Huo J T, Li M C, Chang C T and Sun Y F 2019 *J. Magn. Magn. Mater.* **489** 165404
[303] Vorobiov S, Pylypenko O, Bereznyak Y, Pazuka I, Cizmar E, Orendac M and Komanicky V 2021 *Appl. Phys. A* **127** 179
[304] Huo J T, Huo L S, Men H, Wang X M, Inoue A, Wang J Q, Chang C T and Li R W 2015 *Intermetallics* **58** 31
[305] Huo J T, Huo L S, Li J W, Men H, Wang X M, Inoue A, Chang C T, Wang J Q and Li R W 2015 *J. Appl. Phys.* **117** 073902
[306] Sheng W, Wang J Q, Wang G, Huo J T, Wang X M and Li R W 2018 *Intermetallics* **96** 79
[307] Luo L, Shen H X, Bao Y, Yin H, Jiang S D, Huang Y J, Guo S, Gao S Y, Xing D W, Li Z and Sun J F 2020 *J. Magn. Magn. Mater.* **507** 166856
[308] Zhang Y K, Wu B B, Guo D, Wang J and Ren Z M 2021 *Chin. Phys. B* **30** 017501
[309] Li L W, Xu C, Yuan Y and Zhou S Q 2018 *Mater. Res. Lett.* **6** 413
[310] Dong Z Q, Wang Z J and Yin S H 2020 *Intermetallics* **124** 106879
[311] Zhu W H, Ma L, He M F, Li Z K, Zhang H Z, Yao Q R, Rao G H, Su K P, Zhong X C, Liu Z W and Gao X Q 2023 *Adv. Eng. Mater.* **25** 2201770
[312] Zhang F Q, Wu Z Y, Gong Y, Li W J, Miao X F, Liu J, Xu Y G, Yin W, Lienert U, Eijt S, Wu Z D, Schut H, Gzek J, van Dijk N, Brück E and Ren Y 2024 *Acta Mater.* **300** 121508
[313] Sarlar K, Tekgül A and Kucuk I 2020 *Curr. Appl. Phys.* **20** 18
[314] Sarlar K, Tekgül A and Kucuk I 2019 *IEEE Magn. Lett.* **10** 2109905
[315] Zhang Y K, Zhu J, Hao Z H, Hao W X, Mo Z J and Li L W 2023 *Mater. Des.* **229** 111894
[316] Zhang Y K, Xu P, Zhu J, Yan S M, Zhang J C and Li L W 2023 *Mater. Today Phys.* **32** 101031
[317] Sun Y, Lv W J, Liang Y, Gao Y, Cui W J, Yan Y J, Zhao W Y, Zhang Q J and Sang X H 2023 *Scr. Mater.* **223** 115068
[318] Yin H B C, Law J Y, Huang Y J, Franco V, Shen H X, Jiang S D, Bao Y and Sun J F 2021 *Mater. Des.* **206** 109824
[319] Yin H B C, Law J Y, Huang Y J, Shen H X, Jiang S D, Guo S, Franco V and Sun J F 2022 *Sci. China Mater.* **65** 1134
[320] Yin H, Wang J Q, Huang Y J, Shen H X, Guo S, Fan H B, Huo J T and Sun J F 2023 *J. Mater. Sci. Technol.* **149** 167
[321] Shao L L, Xue L, Luo Q, Yin K B, Yuan Z R, Zhu M Y, Liang T, Zeng Q S, Sun L T and Shen B L 2022 *J. Mater. Sci. Technol.* **109** 147
[322] Xu C J, Jiang X Y, Zou Z G, Xie Z J, Zhang W J and Feng M 2024 *Chin. Phys. B* **33** 127501
[323] Yin Y N, Shi F F, Liu G Q, Tan X J, Jiang J, Tiwari A and Li B H 2022 *Appl. Phys. Lett.* **120** 082404
[324] Law J Y, Moreno-Ramirez L M, Diaz-Garcia A, Martin-Cid A, Kobayashi S, Kawaguchi S, Nakamura T and Franco V 2021 *J. Alloys Compd.* **855** 157424
[325] Law J Y, Diaz-Garcia A, Moreno-Ramirez L M and Franco V 2021 *Acta Mater.* **212** 116931
[326] Zheng Z, Chen X, Wang H Y, Da S, Wang G, Qiu Z, Zeng D and Xia Q 2023 *J. Alloys Compd.* **966** 171483
[327] Guo Y, Zhang T T, Zhang Z S, Chen B, Guo W H, Pan S, Gong Y, Bai Y Q, Gong Y Y, Liu J, Miao X F and Xu F 2022 *APL Mater.* **10** 091107
[328] Batashev I, de Wijs G A and Brück E 2021 *Handbook of Magnetic Materials* **30** 1
[329] Bocarsly J D, Levin E E, Garcia C A C, Schwennicke K, Wilson S D and Seshadri R 2017 *Chem. Mater.* **29** 1613
[330] Garcia C A C, Bocarsly J D and Seshadri R 2020 *Phys. Rev. Mater.* **4** 024402
[331] Hu K, Xie R W, Shen C, Peng H L, Liu H S and Zhang H B 2023 *Acta Mater.* **259** 119255
[332] Zeni C, Pinsler R, Zügner D, Fowler A, Horton M, Fu X, Wang Z L, Shysheya A, Crabbé J, Ueda S, Sordillo R, Sun L X, Smith J, Nguyen B, Schulz H, Lewis S, Huang C W, Lu Z H, Zhou Y C, Yang H, Hao H X, Li J L, Yang C L, Li W J, Tomioka R and Xie T 2025 *Nature* **639** 624
[333] Mo W Q, Wang J F, Yuan G Q, Cao D and Bai G X 2025 *Mater. Today Commun.* **44** 111933
[334] Zhang B, Zheng X Q, Zhao T Y, Hu F X, Sun J R and Shen B G 2018 *Chin. Phys. B* **27** 067503
[335] de Castro P B, Terashima K, Yamamoto T D, Hou Z F, Iwasaki S, Matsumoto R, Adachi S, Saito Y, Song P, Takeya H and Takano Y 2020 *NPG Asia Mater.* **12** 35
[336] Court C J, Jain A and Cole J M 2021 *Chem. Mater.* **33** 7217
[337] Pinto R M C, Belo J H, Araújo J P and Silva D J 2022 *J. Magn. Magn. Mater.* **562** 169706
[338] Silva D J, Ventura J and Araújo J P 2020 *Energy AI* **2** 100030
[339] Maiorino A, Duca M G D, Tomc U, Tusek J, Kitanovski A and Aprea C 2021 *Appl. Therm. Eng.* **197** 117375
[340] Chdil O, Bikerouin M, Balli M and Mounkachi O 2023 *Appl. Energy* **335** 120773
[341] DebRoy T, Wei H L, Zuback J S, Mukherjee T, Elmer J W, Milewski J O, Beese A M, Wilson-Heid A, De A and Zhang W 2018 *Prog. Mater. Sci.* **92** 112
[342] Hou H L, Qian S X and Takeuchi I 2022 *Nat. Rev. Mater.* **7** 633
[343] Liu Y, Li J, Qian Y, Qie S Y, Mi S Y, Xu Z Z, Xie H C, Song X and Ma T Y 2024 *Acta Mater.* **275** 120058
[344] Guo W H, Miao X F, Yan Z B, Chen Y L, Gong Y, Qian F J, Xu F and Caron L 2024 *Mater. Res. Lett.* **12** 315
[345] DebRoy T, Mukherjee T, Wei H L, Elmer J W and Milewski J O 2021 *Nat. Rev. Mater.* **6** 48
[346] Tomc U, Nosan S, Klinar K and Kitanovski A 2023 *J. Adv. Res.* **45** 157